Systematic Entomology

Systematic Entomology (2017), DOI: 10.1111/syen.12276

Morphological variation, genetic differentiation and phylogeography of the East Asia cicada *Hyalessa maculaticollis* (Hemiptera: Cicadidae)

YUNXIANG LIU[1], YUE QIU[1], XU WANG[1], HUAN YANG[1], MASAMI HAYASHI[2] and CONG WEI[1]

[1]Key Laboratory of Plant Protection Resources and Pest Management, Ministry of Education, Entomological Museum, Northwest A&F University, Yangling, China and [2]Laboratory of Entomology, Tokyo University of Agriculture, Atsugi, Japan

Abstract. The cicada *Hyalessa maculaticollis* is widely distributed in East Asia, and is noted for its great morphological variability. The variation in this species and its allies has been a long-standing controversy. The population differentiation, genetic structure and phylogeography of this species are explored based on morphological observations, mitochondrial and nuclear DNA analyses, and comparison of the calling song structure of males. Our results reveal that the abundant intraspecific morphological variations are consistent with high levels of genetic divergence in this species, but incongruence between the morphological variations and genetic divergence is found in a few lineages. Phylogenetic and network analyses indicate that *H. maculaticollis* is composed of two major lineages – China and Japan. The East China Sea (ECS) land bridge acted as a dispersal corridor for *H. maculaticollis* during the glacial period. The climatic oscillations in the Pleistocene and the terrain structure of East Asia influenced population differentiation. The divergence time between the two sides of the East China Sea is estimated to be ~1.05 (95% CI = 0.80–1.30) Ma, which was about the same period during which the sea level increased rapidly during the 'Ryukyu Coral Sea Stage' (0.2–1.3 Ma). Populations of *H. maculaticollis* are structured phylogeographically, with the China populations differentiated into a greater number of highly structured haplogroups. Qinling Mountains and the mountainous regions around the Sichuan Basin are presumed to have been major refugia for *H. maculaticollis* in glacial periods, and a recent population expansion has been detected for populations distributed in the area to the north of Qinling Mountains. The high degree of haplotype and nucleotide diversity shown in East China populations suggests that the flat terrain with low-altitude hills are suitable for the survival of *H. maculaticollis*. The species *H. fuscata*, treated as an independent species from *H. maculaticollis* by some researchers based on acoustic analyses of the calling song structure, is confirmed to be a junior synonym of *H. maculaticollis* based on the results of our analyses of morphological variation, calling song structure and acoustic playback experiments.

Introduction

Past geological events and climatic oscillations have played important roles in forming the contemporary genetic diversity and population structure of animals across the globe (Hewitt, 1996, 2000). In Europe, severe climatic oscillations in the Pleistocene forced many species to either move or go extinct (Hewitt, 1996, 2000, 2004; Avise, 2000); but most areas of East Asia were not glaciated during the Pleistocene (Williams *et al.*, 1998), and the relatively mild Pleistocene climate did not drive many species to undergo any dramatic population change. In addition, the glacial cycles led to sea-level fluctuation. The eastern areas

Correspondence: Cong Wei, Key Laboratory of Plant Protection Resources and Pest Management, Ministry of Education, Entomological Museum, Northwest A&F University, Yangling, Shaanxi 712100, China. E-mail: congwei@nwsuaf.edu.cn

of the Sino-Japanese region, stretching along more than 1500 km in an east–west direction, range from East China to Japan and the Korean Peninsula, and to Taiwan and the Ryukyu Islands (Holt *et al.*, 2013). On account of sea-level fluctuation during the glacial period, the repeated exposure and submergence of the East China Sea (ECS) land bridge played an important role in shaping the population structure of many species (Zhang *et al.*, 2016). Moreover, the mosaic of mountains formed the complex contemporary terrain structure of East Asia. As huge geographical barriers, these mountain systems drove species to gradually adapt to the local environment, reduced the gene flow between different populations and contributed to population differentiation (Li *et al.*, 2009). Mountainous areas also potentially harboured many refugial populations in the ice age, which led to the formation of new lineages/taxa and contributed to a higher genetic diversity (Jiang *et al.*, 2007; Ye *et al.*, 2016). Previous studies of East Asian insects, including *Apocheima cinerarius* (Lepidoptera: Geometridae) (Liu *et al.*, 2015) and *Halyomorpha halys* (Hemiptera: Pentatomidae) (Zhu *et al.*, 2016), have confirmed that Pleistocene climate change had an effect on the distribution and demography these species, which survived in refugia during glacial periods, experienced demographic expansion after the ice age and, eventually, formed their current population structures due to the complex local topography.

Phylogenetics is an efficient approach to assessing genetic structure and diversity of a species population. Studying the spatial genetic structure of a species is crucial to knowing current population genetic processes and predicting the potential of populations to respond to selection and divergent environmental conditions (De Jong *et al.*, 2011; Scarpassa *et al.*, 2015). Phylogenetic methods have been widely applied to various kinds of insects, such as the grass-cutting ant *Acromyrmex striatus* (Cristiano *et al.*, 2016), *Amphiareus obscuriceps* (Hemiptera: Anthocoridae) (Zhang *et al.*, 2016), and some New Zealand and Mediterranean cicadas (Arensburger *et al.*, 2004; Pinto-Juma *et al.*, 2008; Marshall *et al.*, 2009, 2011, 2012), and has provided solid evidence for past biogeographical events.

Their large body size and low dispersal ability make cicadas an excellent group to study phylogeographical patterns and to assess the impact of historical events on the current lineage relationships among different populations (Buckley *et al.*, 2001; Arensburger *et al.*, 2004; Marshall *et al.*, 2008, 2011; Hill *et al.*, 2009; Owen *et al.*, 2016). The cicada *Hyalessa maculaticollis* (Motschulsky) has a very wide distribution, ranging from China to Far East Russia, the Korean Peninsula and into Japan (Chou *et al.*, 1997; Hayashi & Saisho, 2011; Wang *et al.,* 2014). This species is noted for its great intraspecific variability, including markings on thorax and opercula and the shape of aedeagus (Hayashi & Saisho, 2011; Wang *et al.,* 2014). The classification of *H. maculaticollis* and its allies has been a long-standing controversy. This species was formerly put in the genus *Oncotympana* Stål (1870). Chou *et al.* (1997) treated another species, *O. fuscata* (Distant), as a junior synonym of *O. maculaticollis*. Lee (1999) applied the name *O. fuscata* to the Korean population. Lee (2010) described the genus *Sonata*, with *O. fuscata* as the type species, and transferred nine species of *Oncotympana* occurring in continental East Asia, Japan and India to *Sonata*, among which *O. maculaticollis* was included. However, Hayashi (2011) synonymised *Sonata* Lee with *Hyalessa* China, 1925, and transferred *S. maculaticollis* to *Hyalessa*. Hayashi & Saisho (2011) recognized *S. fuscata*, the type species of *Sonata*, as a junior synonym of *H. maculaticollis*. Wang *et al.* (2014) also treated *H. fuscata* as a junior synonym of *H. maculaticollis*, and found that the population of *H. maculaticollis* collected from Mt. Nanwutai, Xi'an, China differs from other populations by its S-shaped aedeagal shaft. But they tentatively treated related specimens as a variant of *H. maculaticollis*. Recently, Puissant & Lee (2016) conducted acoustic analyses of the calling song structure of '*H. fuscata*' occurring in South Korea, comparing it with that of *H. maculaticollis* distributed in Japan, and concluded that the acoustical differences between them indicated that *H. fuscata* is an independent species. However, *H. fuscata* (the former *O. fuscata*) was described from North China (Distant, 1905), yet the analysis in Puissant & Lee (2016) did not involve any populations of *H. maculaticollis* occurring in China. Determining the degree of population differentiation and phylogeography of *H. maculaticollis* is important in order to clarify the identity of this species and its allies.

In the present study, the morphological variations, genetic differentiation and phylogeography of various populations of *H. maculaticollis* collected from China and Japan are examined. The morphology of *H. maculaticollis* is compared with that of the holotype of *H. fuscata* as well as the population occurring in South Korea, which was treated as *H. fuscata* by Lee (1999) and Puissant & Lee (2016). In addition, the calling song structure of three representative populations occurring in China is studied and compared with those of related populations from Japan and the Korean Peninsula, and acoustic playback experiments are conducted to further clarify whether these populations belong to the same species. Our results advance understanding of morphological and genetic differentiation and phylogeography of this widely distributed cicada species, and will be valuable in future studies of phylogeography and evolution of other related cicadas occurring in East Asia.

Material and methods

Sample preparation

In total, 216 specimens of *H. maculaticollis* were collected across mainland China and in Japan for molecular studies (Fig. 1). One hind leg of fresh material from each specimen was immediately preserved in 100% ethanol and stored in a −80°C refrigerator until they were used in DNA extraction. The species *H. ronshana* China, *H. stratoria* (Distant) and *H. wangi* Wang, Qiu & Wei were selected as the outgroups in the phylogenetic analysis and also to determine the interspecies genetic distance. All specimens used for molecular identification and phylogenetic analysis are listed in Table 1.

Voucher specimens of *H. maculaticollis* were deposited in the Entomological Museum, Northwest A&F University (NWAFU), Yangling, China.

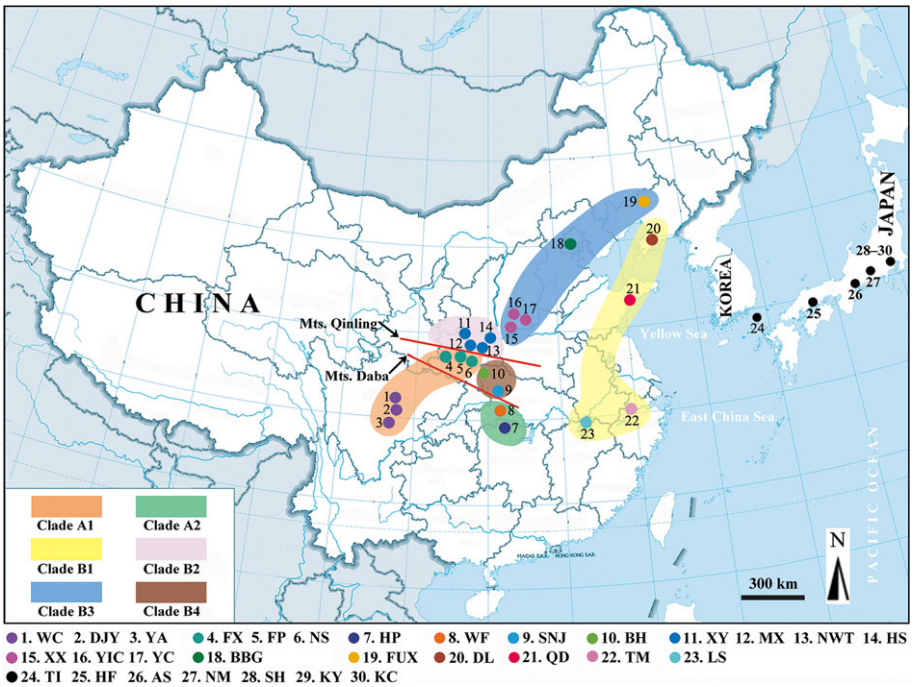

Fig. 1. Distribution of *Hyalessa maculaticollis*. Numbers with coloured dots represent sampling sites. Translucent colour areas represent different haplogroups as in Fig. 6. Related star-studded mountains are marked schematically with red lines. [Colour figure can be viewed at wileyonlinelibrary .com].

Morphology

The external morphology of the specimens was examined using an Olympus SZX10 stereomicroscope (Olympus Corporation, Tokyo, Japan) and photographed using a Canon PowerShot SX60HS digital camera (Canon Corporation, Japan). The pygofer was dissected from the terminal abdominal segments, then placed in 10% KOH and boiled for 2–5 min, washed, and transferred to glycerin for observation. The aedeagus was photographed using a Scientific Digital micrography system equipped with an Auto-montage imaging system and a QIMAGING Retiga 4000R digital camera (CCD) (QImaging, Surrey, BC, Canada). Then morphological comparison was conducted among various populations of *H. maculaticollis* collected from China and Japan and the holotype of *H. fuscata* as well as the population of *H. fuscata* occurring in the Korean Peninsula (KOR). All measurements were recorded in mm. The terminology for morphological features follows that of Moulds (2005, 2012).

DNA extraction, PCR and sequencing

Total genomic DNA was extracted from leg muscle using a Biospin Insect Genomic DNA Extraction Kit (Bioer Technology Co., Ltd, Hangzhou, China) following the manufacturer's instructions. Standard PCR methods were used to amplify partial sequences of two nuclear genes (the elongation factor-1 alpha gene (*EF-1α*) and internal transcribed spacer (*ITS*)), and three mitochondrial genes (cytochrome c oxidase subunit I (*COI*), cytochrome c oxidase subunit II (*COII*) and cytochrome b (*Cytb*). PCR primers are listed in Table 2 and amplifications were conducted in a total volume of 25 μL using the following thermal cycling conditions: an initial denaturing step at 94°C for 5 min; 34 cycles of denaturing at 94°C for 30 s; annealing at 56, 59.3, 51.4, 52.3 and 41.9°C for 1 min for *EF-1α*, *ITS*, *COI*, *COII* and *Cytb*, respectively; an extension at 72°C for 1 min; and a final extension step of 72°C for 10 min. The PCR products were electrophoresed in 1.0% agarose gel staining with ethidium bromide to ensure the products were the target fragments we needed. DNA products were subsequently sequenced by Sangon Biotech (Shanghai) Co., Ltd, using PCR primers. All new sequences have been submitted to GenBank (Accession Nos.: *COI*: KY860146–KY860361; *Cytb*: KY912386–KY912597; *COII*: KY885250–KY885465; *ITS*: KY886809–KY886890; *EF-1α*: KY929019–KY929100). In addition, 16 *COI* sequences of Japanese populations (NM, KY, AS, HF) were downloaded from GenBank for subsequent research.

Molecular data analysis

Sequence chromatograms were checked carefully using Chromas Pro software (Technelysium Pty Ltd., Australia). Multiple sequences were aligned in CLUSTAL X v2.0.21 (Thompson *et al.*, 1997; Jeanmougin *et al.*, 1998); subsequently the gappy columns at the beginning and end of the alignment were manually deleted with BIOEDIT v7.0.9.0 (Hall, 1999), and were then

Table 1. Samples of *Hyalessa maculaticollis* and related species (*H. ronshana*, *H. stratoria* and *H. wangi*) used for molecular analyses in this study.

Species	Population	Locality	Collecting date/GenBank accession Nos.
H. maculaticollis	YA	Ya' an City, Sichuan Province, China	28 July 2013
	DJY	Dujiangyan City, Sichuan Province, China	9 August 2013
	WC	Wenchuan County, Sichuan Province, China	1 August 2013
	FX	Fengxian County, Shaanxi Province, China	9 August2015
	FP	Foping County, Shaanxi Province, China	16 July 2014
	NS	Ningshan County, Shaanxi Province, China	5 August 2012
	HP	Mt. Huping, Shimen County, Hunan Province, China	26 July 2013
	WF	Wufeng County, Hubei Province, China	12 July 2015
	SNJ	Mts. Shennongjia, Hubei Province, China	11 August 2004
	BH	Baihe County, Shaanxi Province, China	20 August 2010
	XY	Xunyi County, Shaanxi Province, China	10 August 2015
	MX	Meixian County, Shaanxi Province, China	18 August 2014
	NWT	Mt. Nanwutai, Xi' an City, Shaanxi Province, China	14 August2014
	HS	Mt. Huashan, Huayin City, Shaanxi Province, China	29 July 2014
	YC	Yangcheng County, Shanxi Province, China	30 July 2012
	YIC	Yicheng County, Shanxi Province, China	19 July 2012
	XX	Xiaxian County, Shanxi Province, China	25 July 2012
	BBG	Beijing Botanical Garden, Beijing City, China	8 July 2015
	FUX	Fuxin City, Liaoning Province, China	14 July 2014
	DL	Dalian City, Liaoning Province, China	26 July 2015
	QD	QingdaoCity, Shandong Province, China	29 July 2010
	TM	Mt. Tianmushan, Lin'an City, Zhejiang Province, China	9 July 2014
	LS	Mt. Lushan, Lushan City, Jiangxi Province, China	18 July 2013
	TI	Tsushima Island, Kyushu, Japan	6 August 2003
	SH	Saitama, Saitama Pref., Honshu, Japan	14 August 2008, 29 August 2009
	KC	Chigasaki, Kanagawa Pref., Honshu, Japan	31 July 2016
	NM	Matsumoto, Nagano Pref., Honshu, Japan	AB900922–AB900926
	KY	Yokohama, Kanagawa Pref., Honshu, Japan	AB900123–AB900125
	AS	Seto, Aichi Pref. Honshu, Japan	AB900914–AB900918
	HF	Fukuyama, Hiroshima Pref., Honshu, Japan	AB898798–AB898800; AB900118–AB900119
H. ronshana	–	Yulong Naxi Autonomous County, Yunnan Province, China	7 August 2010
H. stratoria	–	Dali City, Yunnan Province, China	20 August 1980
H. wangi	–	Shuangjiang County, Yunnan Province, China	22 August 2015

Sequences of populations NM, KY, AS and HF were downloaded from GenBank.

Table 2. Primer names, sequences used in PCR reactions of the genes sequenced.

Primer for gene	Primer name	Primer sequence 5′–3′	References
COI	LCO1490	GGTCAACAAATCATAAAGATATTGG	Simon *et al.* (1994)
	HCO2198	TAAACTTCAGGGTGACCAAAAAATCA	
Cytb	CB1	TATGTACTACCATGAGGACAAATATC	Simon *et al.* (1994)
	CB2	ATTACACCTCCTAATTTATTAGGAAY	
COII	COII–3037	TAGTATGGCAGATTAGTGCAATGAA	Zahniser & Dietrich (2015)
	COII	CCRCAAATTTCWGARCATTGACCA	
EF-1α	EF1–PA–f650	TGCTGCGGGTACTGGTGAAT	Arensburger *et al.* (2004)
	EF1–N–1419	ACACCAGTTTCAACTCTGCC	
ITS	CAS5p8sB1d	ATGTGCGTTCRAAATGTCGATGTTCA	Ji *et al.* (2003)
	CAS18sF1	TACACACCGCCCGTCGCTACTA	

translated into amino acids for confirmation of the alignment using PRIMER PREMIER v5 (Lalitha, 2000). Because no repeatable criteria were invoked in the determination of which regions were divergent or ambiguously aligned in the manual alignment using BIOEDIT, the alignment used for phylogenetic analyses was tested for its sensitivity to misaligned regions identified using the program GBLOCKS (Castresana, 2000). The level of substitution saturation of each gene and each codon position of each protein-coding gene was tested using DAMBE v5.3.74 (Xia, 2013). Pairwise corrected genetic distances of the *COI* gene for all species were calculated using MEGA v6.05 (Tamura *et al.*, 2013). The haplotypes were defined using DNASP v5.0 (Librado & Rozas, 2009) based on the mitochondrial genes and nuclear genes. Genetic diversity was estimated using DNASP v5.0 by computing haplotype diversity (H) and nucleotide diversity (π).

The most suitable partitioning strategies and the respective evolution models for each partition were estimated based on the program PARTITIONFINER v1.1.1 (Lanfear *et al.*, 2012) by giving the program different potential groups of first, second and third codon positions of the protein-coding genes and the ribosomal RNA gene. The Bayesian Information Criterion (BIC) was used to compare alternative partitioning schemes and sequence models. For the concatenated data of *COI*, *COII*, *Cytb*, *EF-1α* and *ITS*, the optimal partitions and models were as follows: *ITS* with TVM + G; first codon position of *COI*, *COII* with HKY + I + G; second codon position of *COI* with F81; second codon position of *Cytb* and *EF-1α* with HKY + I; and third codon position of *COI*, *Cytb* and *EF-1α* with HKY + G. The combined *COI*, *COII* and *Cytb* dataset was divided into two partitions, first and second codon positions of *CO1* and *COII* with HKY + I + G, third codon position of *COI* and *Cytb* with TrN + I. The optimal model of three codon positions in *COI* gene was F81 + G.

The phylogenetic relationships within the mainland China populations were reconstructed using all haplotypes of the complete mtDNA dataset. The phylogenetic trees of all East Asia populations – mainland China and Japan – were reconstructed based on haplotypes of all mtDNA and nuclear datasets together. We also reconstructed the phylogenetic relationships of all East Asia populations with *COI* genes. The trees were constructed using maximum-likelihood (ML) implemented in PHYML v3.0 (Guindon & Gascuel, 2003) and Bayesian inference (BI) using MRBAYES v3.1.2 (Ronquist & Huelsenbeck, 2003). All ML analyses with thorough bootstrap were run ten times starting from random seeds under the GTR + I + G model. The bootstrap support (BS) value was determined by analysis with 1000 replicates. We produced posterior probability distributions by allowing four incrementally heated Markov chain Monte Carlo (MCMC) chains (one cold chain and three hot chains) to proceed for 5 million generations, with sampling done every 100 generations for yielding 50 000 trees. The average standard deviation of split frequency was lower than 0.01, indicating that the sampling of posterior distribution was adequate. The average standard deviation of split frequencies and Potential Scale Reduction Factor (PSRF) were used for examining convergence. The stationarity was determined with the program TRACER v1.5 (Rambaut & Drummond, 2009) by plotting the log-likelihood values versus generation number. A common methodology to check the convergence is by tracking the Gelman–Rubin convergence statistic as modified by Brooks & Gelman 1998. After the first 25% of the yielded trees were discarded as burn-in, a 50% majority-rule consensus tree with the posterior probability values was constructed by summarizing the remaining trees.

The network profile of the haplotypes identified in *H. maculaticollis* was constructed with NETWORK v5.0 (Bandel *et al.*, 1999) using the median-joining method. The data for the three mitochondrial genes and two nuclear genes were concatenated for analysis of mainland China populations, respectively, including the *COI* gene for all East Asia populations.

Based on the previous analysis, we divided the populations into haplogroups. A three level hierarchical AMOVA was estimated by the genetic variation and fixation indices implemented in ARLEQUIN v3.5 (Excoffier & Lischer, 2010) by computation of conventional *F*-statistics from haplotypes with 1000 permutations.

We calculated Tajima's *D* and Fu's *F* statistic and ran 10 000 coalescent simulations for each statistic to create 95% confidence intervals in order to investigate the historical population demographics and test whether the sequences conformed to the expectations of neutrality. Pairwise mismatch distribution analyses were performed to find the evidence of past demographic expansions using DNASP v5.0.

The divergence time analysis of *H. maculaticollis* was estimated using BEAST v1.8.0 (Drummond & Rambaut, 2007) based on *COI* genes. Because no fossil or geological evidence was available for calibration in Cicadidae, we used the widely accepted molecular clock of the mtDNA gene. Although the use of a molecular clock as the only way for calibrating phylogenetic trees is controversial, it does provide a method for estimating approximate divergence times when no other calibration information is available (Maekawa *et al.*, 2001; Hill *et al.*, 2009; Marshall *et al.*, 2009, 2012; Owen *et al.*, 2016). Thus, in this study the proposed conventional mutation rates for the insect mitochondrial *COI* gene of 2.3% per million years (i.e. 0.0115 substitutions/site per lineage) were used (Brower, 1994). The *COI* gene was assigned a relaxed clock model in the analysis. Default priors were used. Chains were analysed for 200 million generations, with sampling every 100 generations. TRACER was used to verify the posterior distribution and the effective sample sizes (ESSs) from the MCMC output. We used TREEANNOTATOR v1.8.0 in the BEAST package to summarize tree data with 'mean height' and discarded the first 25% of trees as the 'burn-in' period, which ended well after the stationarity of the chain likelihood values were established. The tree and divergence time were displayed in FIGTREE v1.3.1.

Calling song structure analyses and comparison of H. maculaticollis

We obtained male calling songs, at an average temperature around 35°C, from three sites: 11 samples in the field on 06 August 2016, at Tangyu Valley, Meixian (MX) County, Shaanxi Province; six samples in the field on 15 July 2017, at Tianmu (TM) Mountain, Zhejiang Province; and 13 samples in the field on 18 July 2017, at Qingdao (QD), Shandong Province, China. All acoustic recordings were made using a linear PCM recorder with stereo microphones (PCM-D100, Sony, China; frequency range 20–20 000 Hz and a 44.1 kHz/16 bit sampling resolution). The sounds were recorded in .WAV file format, and stereo recordings were converted to mono at a sampling rate of 44.1 kHz and resolution of 16 bits. Acoustic analysis was conducted using RAVEN PRO v1.4 (The Cornell Lab of Ornithology, Ithaca, NY, U.S.A.) and SEEWAVE (Sueur *et al.*, 2008), a custom-made library of the R software platform (R Development Core Team, 2011). Terminology for the description of acoustic signals follows that of Puissant & Sueur (2010).

The frequency domain and duration of calling songs of the above three populations were compared with samples from

South Korea (KOR) (data from Puissant & Lee, 2016) and Japan (JAP) (data from Hayashi & Saisho, 2011). In the frequency domain, the dominant frequencies (F1, F2, F3 and F4) were measured using a fast Fourier transform (FFT) with 44.1 Hz precision. For duration, calling songs of MX, TM, QD, KOR and JAP populations were compared with each other. We conducted ANOVAs to examine the dominant frequency and duration of parts of calling songs among different populations, followed by a Student–Newman–Keuls test. All statistical analyses were performed using IBM SPSS Statistics v20.0 (IBM Corp, Armonk, NY). In all tests, significance was assessed at $\alpha = 0.05$, and results were reported as mean ± SD.

Acoustic playback experiments

Our primary results of acoustic analysis indicated that no significant differences were found between the QD and KOR populations (see Results), of which the latter was treated as *H. fuscata* instead of *H. maculaticollis* by Lee (1999) and Puissant & Lee (2016). Our field investigations also found that, similar to many other cicada species, when a male of *H. maculaticollis* began to call, more and more surrounding males in the population followed (chorusing behaviour). To further clarify whether these related populations belong to the same species, acoustic playback experiments were carried out in natural conditions to examine the response of QD population males to acoustic stimuli from the MX population and also that of MX population males to acoustic stimuli from the QD population, respectively. Acoustic stimuli from the MX population were recorded on 06 August 2017, and those from the QD population were recorded on 15 July 2017. These acoustic stimuli were generated at a sample rate of 44.1 kHz and 16-bit resolution with the R package SEEWAVE (Sueur *et al.*, 2008), and played back using a Sony PCM-D100 Linear PCM Recorder and a Mogic Q2 loudspeaker (frequency response, 150–20 000 Hz). For each type of sound stimulus, 13 males were tested, and no cicada was tested more than once with any one experimental stimulus. The two types of acoustic stimuli were then played back for 5 min duration in random order from a loudspeaker placed ~2 m from the males. During the playback of each sound stimulus, we recorded the number of sounds produced by the males in response. After each test, we moved to another site and conducted a new playback experiment with a different male. The observations were made between 10:00 am and 16:00 pm, a period that corresponded to the peak acoustic activity of this cicada species. During the experiments, the ambient temperature ranged from 30 to 35°C. Fisher's exact test was used to detect differences in the percentage of responding males.

Results

Morphological variations of H. maculaticollis *and related '*H. fuscata*'*

Hyalessa maculaticollis shows considerable variation in markings on mesonotum and opercula of males, and in the shape of the aedeagus. The variations in the markings on the mesonotum of males include the following four types: (i) mesonotum with five pairs of greenish spots – a pair of very small ones near anterior margin, three large spots on disc, and a pair of very large spots on lateral margins (Fig. 2; YA, DJY, WC, FX, FP, NS, WF, HP, DL, QD, LS3, TM2, HS2, MX1, YC2, YIC2, BBG, FUX, BH, SNJ, TI, SH1); (ii) mesonotum with five pairs of spots obscure or reduced (Fig. 2; LS2, TM1, MX2, NWT, YC1); (iii) mesonotum with no distinct markings on disc (Fig. 2; LS1, HS1, YIC1, XX); and (iv) two large spots on disc that change into stripes and connect together with the spots on lateral margins, and cover most of the area of the mesonotum (Fig. 2; SH2). Three types of variations are found in the opercula of males: (i) black opercula (Fig. 3; YA, DJY, WC, FX, FP, NS, WF, HP, BH, SNJ); (ii) variegated opercula (Fig. 3; TM, LS, SH); and (iii) brown opercula (Fig. 3; DL, QD, HS, MX, NWT, BBG, YC, YIC, XX, FUX, TI). Three types of variations of aedeagal shaft are observed: (i) aedeagal shaft slightly S-shaped in lateral view (Fig. 4; FX); (ii) aedeagal shaft S-shaped in lateral view (Fig. 4; LS, MX, YC, BH); and (iii) aedeagal shaft C-shaped in lateral view (Fig. 4; FUX).

The holotype of *H. fuscata* and males from South Korea (KOR) that were treated as *H. fuscata* by Puissant & Lee (2016) possess five pairs of greenish spots on the mesonotum, which is consistent with variation (i) (Fig. 2). The colour of male opercula (Fig. 3) as well as the shape of aedeagus (not shown in this study) of the so-called *H. fuscata* are also consistent with the variations of *H. maculaticollis*.

Population structure and phylogenetic relationships of H. maculaticollis

In total, 1641 unambiguous base pairs of mitochondrial genes (639 bp of *COI*, 420 bp of *Cytb*, 582 bp of *COII*) were sequenced, and no stop codon was observed. For the nuclear gene dataset, 1431 bp (825 bp of *ITS*, 606 bp of *EF-1α*) were sequenced.

For the mainland China populations, we identified 43 haplotypes of mtDNA genes and 20 haplotypes of nuclear genes (Table 3). Haplotype networks of the populations were constructed (Fig. 5). For the mtDNA genes (Fig. 5A), two haplotypes (H21, H31) were shared by several populations, and 41 haplotypes were private (unique to a single population). The haplotypes were obviously differentiated into two major clades, A and B. Clade A comprises two haplogroups: Clade A1 (populations HP and WF) and Clade A2 (populations YA, DJY, WC, FX, FP, NS) (see Fig. 1). Clade B consists of four haplogroups: (i) Clade B1 (populations DL, QD, TM and LS); (ii) Clade B2 (populations XY, MX, NWT and HS); (iii) Clade B3 (populations of YC, YIC, XX, BBG and FUX); and (iv) Clade B4 (populations SNJ and BH). However, the nuclear genes (Fig. 5B) showed lower intraspecific polymorphism, and the population differentiation is not obvious. Thus, all of the following analyses were performed only with the mtDNA genes.

Based on the combined mtDNA dataset, we reconstructed phylogenetic trees with different methods for the mainland

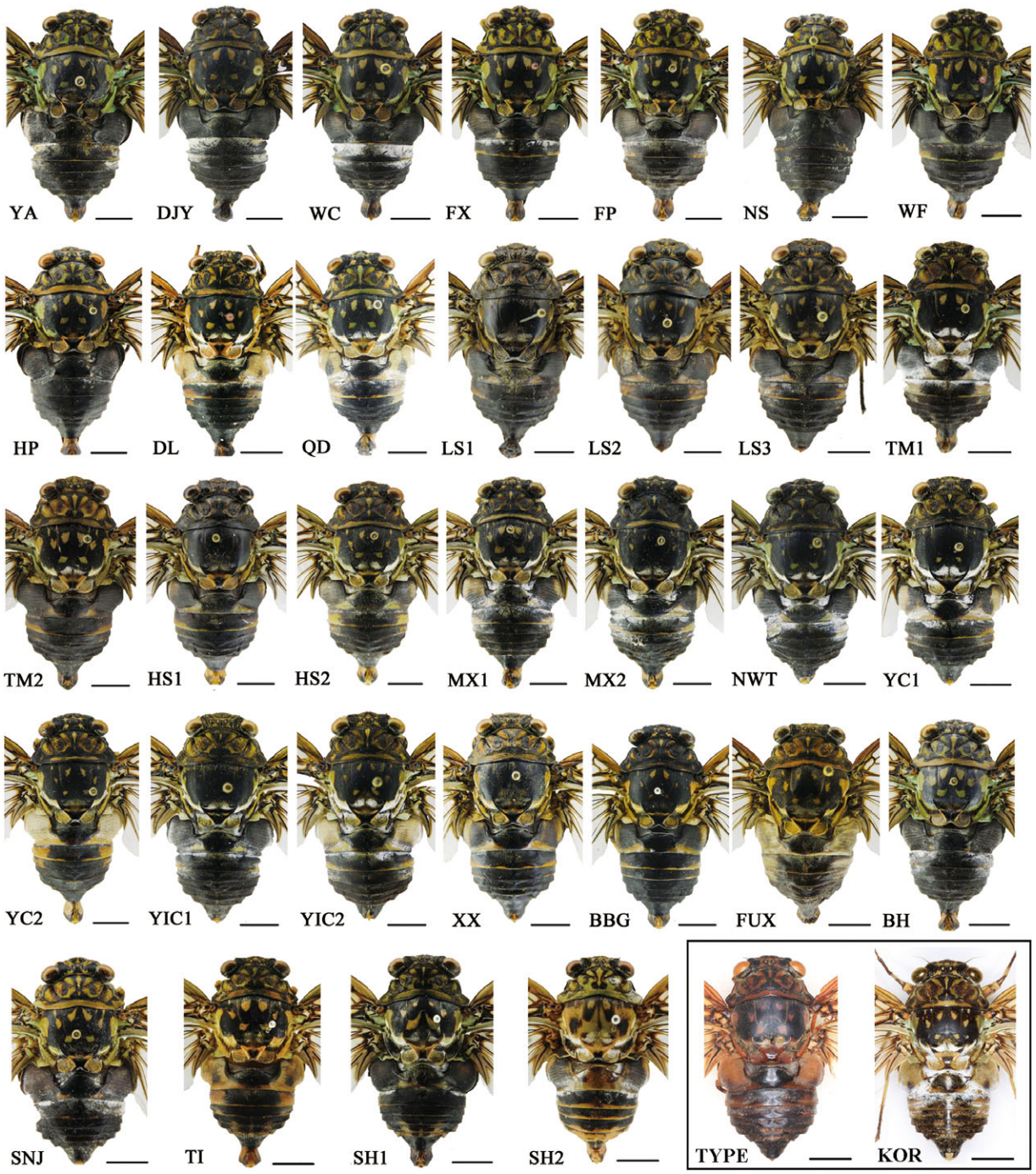

Fig. 2. Variations of the markings on the mesonotum of *Hyalessa maculaticollis* populations, the holotype (TYPE) and the Korean Peninsula population (KOR) of *H. fuscata*. Scale bars, 5.0 mm. [Colour figure can be viewed at wileyonlinelibrary.com].

China populations, and the ML topology was consistent with the Bayesian topology (Fig. 6). The best-fit model in ML analysis was GTR + I + G, and the best model in BI analysis was HKY + G. Moreover, the support values in the BI tree were generally higher than those in the ML tree, and all of the major nodes have >70% BI bootstrap support in the tree. The results of both ML and BI trees separated *H. maculaticollis* populations into two major clades and six haplogroups – Clade A (Clade A1–A2) and Clade B (Clade B1–B4). This is consistent with the haplotype network results (Fig. 5A, B).

Results from the AMOVA for the mainland China populations showed that the overall genetic variation among the six

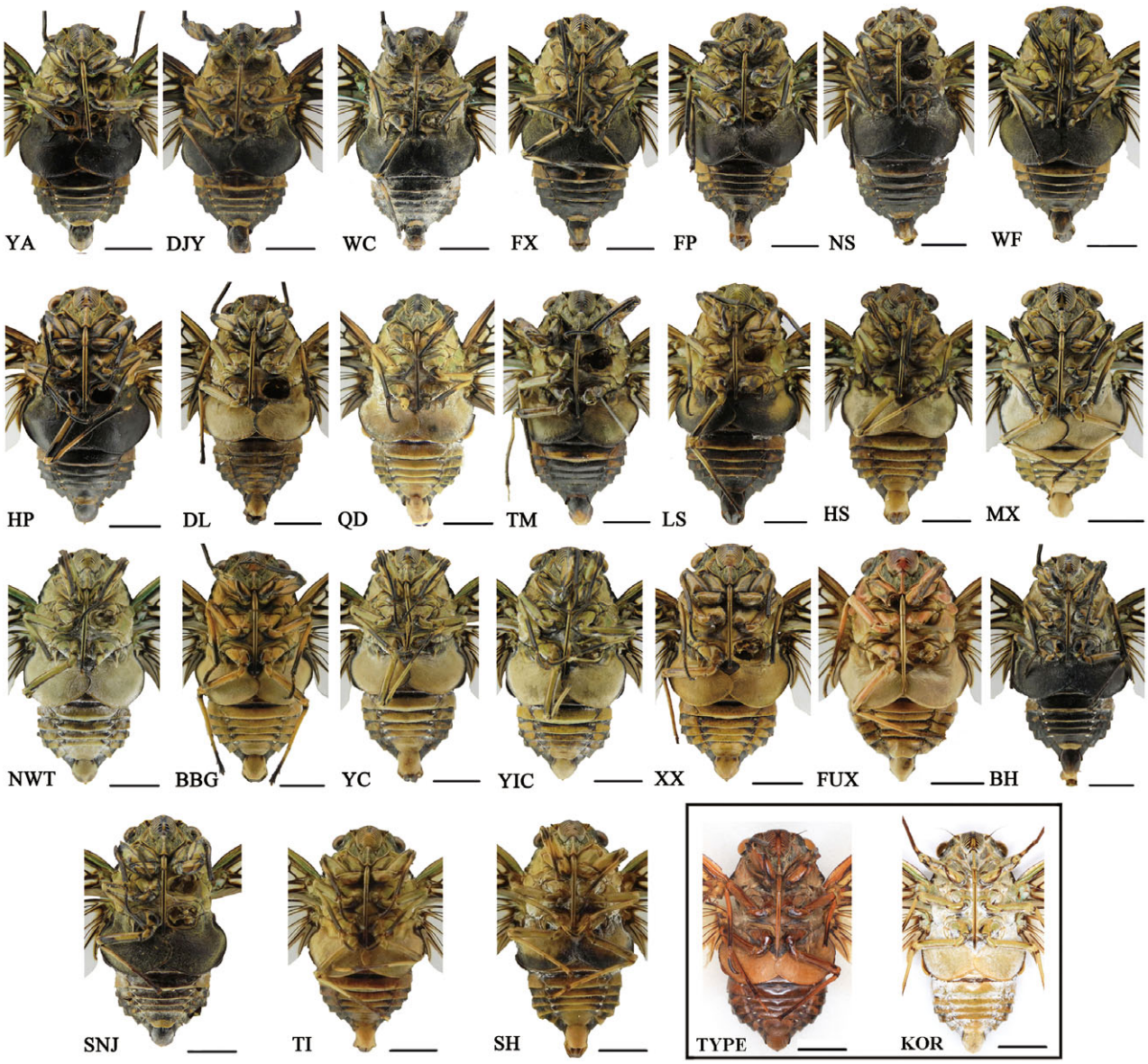

Fig. 3. Variations of the male opercula of *Hyalessa maculaticollis* populations, the holotype (TYPE) and the Korean Peninsula population (KOR) of *H. fuscata*. Scale bars, 5.0 mm. [Colour figure can be viewed at wileyonlinelibrary.com].

haplogroups was 81.83%, whereas it was only 12.81% among populations within haplogroups, and 5.36% within populations (Table 4). The fixation index was high and statistically significant. The AMOVA results showed that most of the genetic variation was attributed to differences among haplogroups.

We further used *COI* sequences to analyse the population structure of all of the mainland China populations and the Japanese populations. The network (Fig. 7) showed that the populations of Japan (Clade C) were obviously different from the mainland China populations, and the AMOVA results showed that the genetic variation among the haplogroups was 87.03% (Table 4).

The phylogenetic trees were reconstructed for all East Asia populations based on joint mitochondrial genes and nuclear genes. The best-fit model selected for ML analysis was GTR + I + G, and the best model in BI analysis was HKY + I + G. The ML topology was consistent with the Bayesian topology (Figure S1). We also reconstructed phylogenetic trees for all East Asia populations based on the *COI* gene (Figure S2). The best-fit model selected for ML analysis was GTR + I + G and that for the BI analysis was F81 + G. The ML topology was also consistent with the Bayesian topology (Figure S2). The topological structure based on the *COI* gene was consistent with the network, and was roughly the same

Fig. 4. Variations of the aedeagus of *Hyalessa maculaticollis* populations. Scale bars, 1.0 mm. [Colour figure can be viewed at wileyonlinelibrary .com].

Table 3. List of the haplotypes of *Hyalessa maculaticollis* with different genes.

Populations	*COI* + *COII* + *Cytb*	*EF-1α* + *ITS*	*COI*	*COI* + *COII* + *Cytb* + *EF-1α* + *ITS*
YA	H34, H35	H7	H1, H5	H2, H6
DJY	H31	H6, H7	H3	H1
WC	H31, H32	H7	H3, H4	H1, H5
FX	H30, H33	H6, H7	H1, H2	H4, H6
FP	H31, H37	H7	H3, H5, H7	H1, H7
NS	H35, H36	–	H5, H6	H2, H3
HP	H40, H41, H42, H43	H4	H10, H11	H10, H11
WF	H38, H39	H1,H3, H4	H8, H9	H8, H9
SNJ	H11, H12, H13	–	H12, H13	H20, H21
BH	H14	–	H14	H22
XY	H15, H17	H9, H10	H25, H26	H12, H19
MX	H16, H17, H27, H28	H2, H5, H7, H8, H12	H25, H27, H28	H12, H18
NWT	H17, H29	H5	H25, H30	H12, H16
HS	H17	H2, H5, H11, H12, H21	H25	H12
YC	H19, H21	H13, H14	H25	H12
YIC	H18, H21, H23, H25	H13, H14	H23, H25, H29	H12, H13, H15
XX	H21, H24, H26	H13	H24, H25	H12, H14
BBG	H20, H21	H13	H25	H12
FUX	H21, H22	H15, H16, H17, H18	H25	H12
DL	H1, H2	H18	H15, H16	H25, H26
QD	H3, H4	–	H17, H18	H23, H24
TM	H5, H6	H18	H19, H20	H27, H28
LS	H7, H8, H9, H10	H7, H19	H21, H22	H29, H30
TI	–	–	H17	H24
SH	–	–	H31	H31
KC	–	–	H31, H32	H31, H37
NM	–	–	H31, H33	H31, H32
KY	–	–	H31	H31
AS	–	–	H31, H34	H31, H33
HF	–	–	H35, H36, H37	H34, H35, H36

See Table 1 for population localities.

as the trees reconstructed using joint mitochondrial genes and nuclear genes (Figure S1).

Diversity indices

Mitochondrial genetic diversity indices for the six haplogroups of mainland China populations of *H. maculaticollis* are presented in Table 5. The number of haplotypes within haplogroups ranged from four (Clade B4) to ten (Clade B1). The haplotype diversity was large, ranging from 0.308 (Clade B2) to 0.894 (Clade B1). The nucleotide diversity ranged from 0.00027 (Clade B2) to 0.00465 (Clade B1).

Demographic analysis

Neutrality tests were conducted for each of the six mainland China haplogroups of *H. maculaticollis* with the combined mtDNA dataset (Table 5). Among the six haplogroups, Clade B3

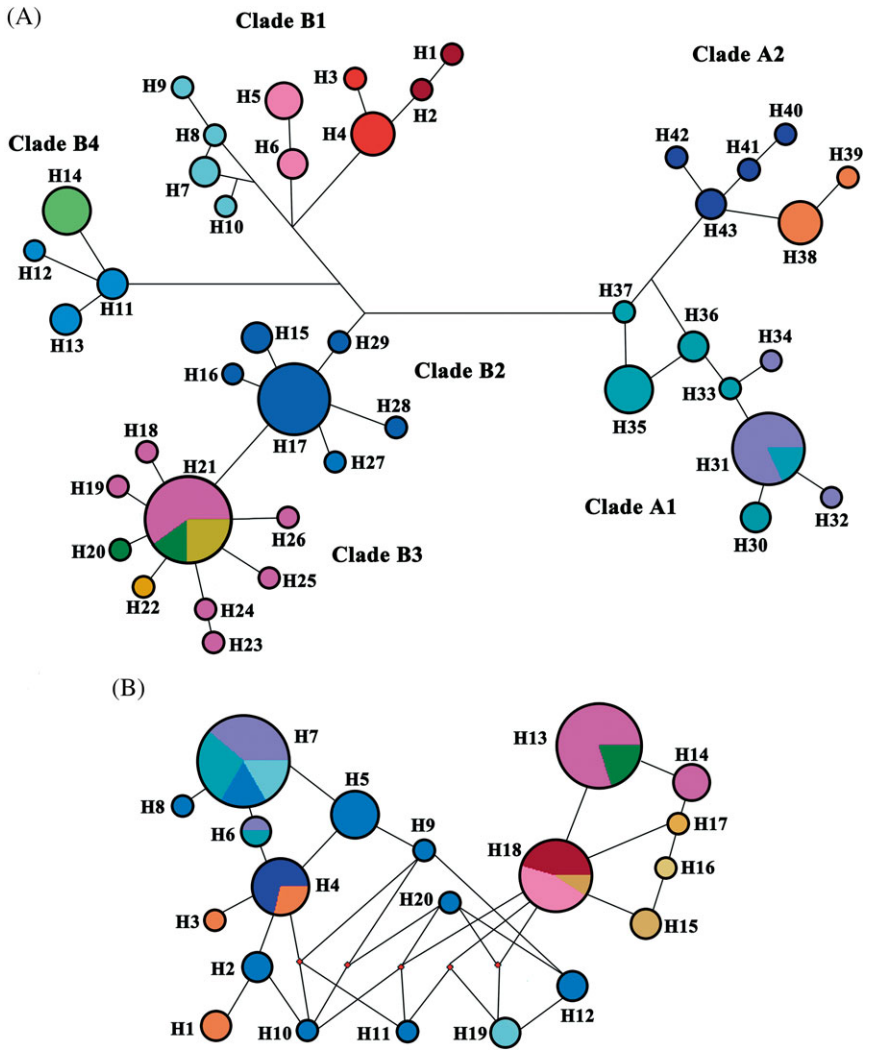

Fig. 5. Network profile of mainland China populations. (A) Network profile based on mtDNA genes; (B) network profile based on nuclear genes. Each haplotype is represented by a circle. The size of the circle is proportional to that haplotype's frequency. Colours denote lineage membership and are the same as in Fig. 1. [Colour figure can be viewed at wileyonlinelibrary.com].

showed significant, negative values for both Fu's F_s ($P < 0.01$) and Tajima's D ($p < 0.05$) tests, and Clade B2 showed significant, negative values for Tajima's D ($P < 0.05$) tests. These results show that clades B2 and B3 significantly reject the hypothesis of neutral evolution, indicating that recent population expansion has occurred within these lineages. The unimodal curves found with the mismatch distribution provided the same inference as neutrality tests – a population expansion (Fig. 8A, B). The star-like structures of the haplotype network also corroborate these results (Fig. 5A).

Estimation of divergence time

The result of divergence time is shown in Fig. 9. The divergence occurred in populations between mainland East Asia (clades A1–A2 and B1–B4) and Japan (Clade C) at ~1.05 (95% CI = 0.78–1.32) Ma. Subsequently, the divergence that occurred in ~0.71 (95% CI = 0.61–0.81) Ma led the mainland China populations to separate into two clades: A1–A2 and B1–B4. The separation of Clade A1 and Clade A2 took place at ~0.52 (95% CI = 0.38–0.66) Ma; and Clade B1, Clade B2 + B3, and Clade B4 diverged at ~0.50 (95% CI = 0.35–0.65) Ma. In the late Pleistocene (0.01–0.12 Ma), a small degree of genetic differentiation appeared in all of the populations; we do not show all of the specific times of divergence.

Intraspecific genetic distance of H. maculaticollis *and interspecific genetic distance between* Hyalessa *species*

The pairwise corrected genetic distances based on *COI* sequences of *H. maculaticollis* and other *Hyalessa* species are shown in Table 6. Intraspecific genetic distances (0.000–0.044)

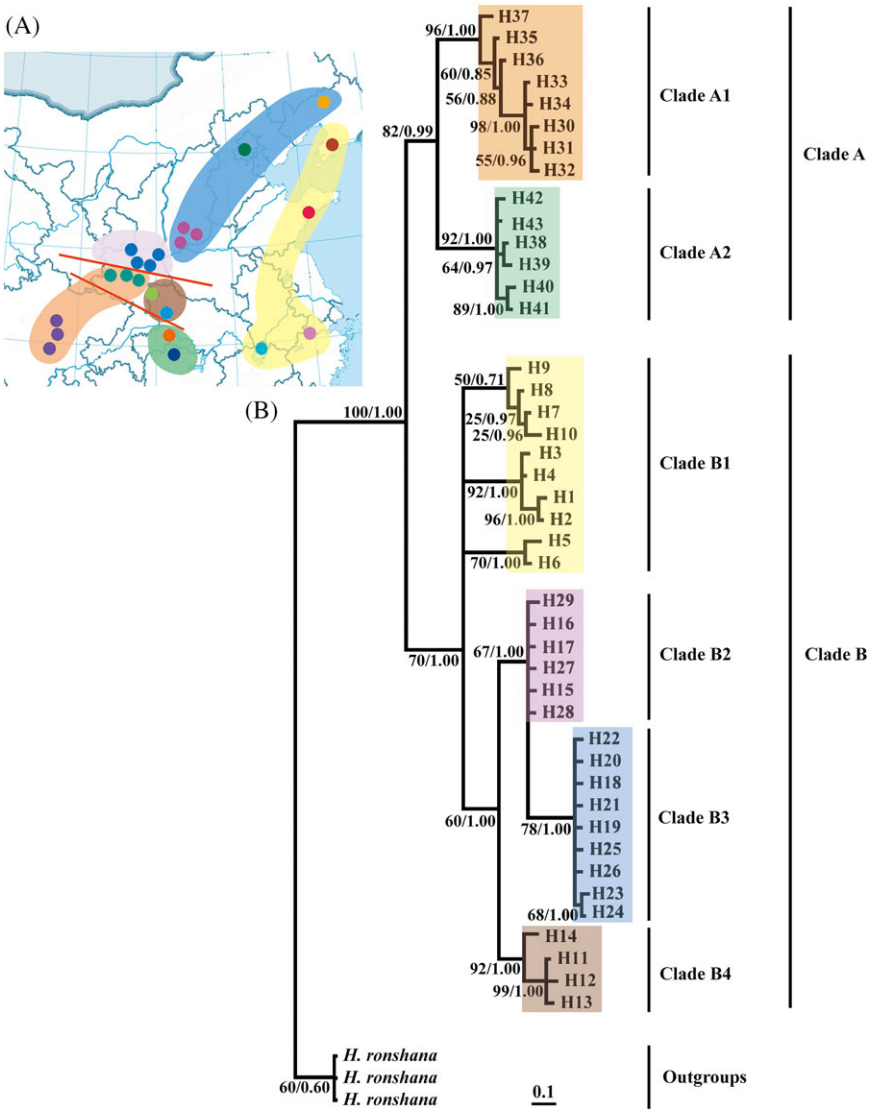

Fig. 6. Phylogenetic tree and the map of distribution of China populations. (A) Distribution of *Hyalessa maculaticollis* in mainland China; (B) phylogenetic tree of mainland China populations based on the mtDNA dataset. Nodal values near branches indicate bootstrap supports and posterior probabilities of maximum-likelihood/Bayesian inference. [Colour figure can be viewed at wileyonlinelibrary.com].

for *H. maculaticollis* are distinctly lower than those between *Hyalessa* species (0.068–0.132), without overlap. This indicates that the variations between different populations of *H. maculaticollis* have not reached species level. Among the populations of *H. maculaticollis*, the intraspecific genetic distances between Clade C and the mainland clades are the highest (Table 6).

Calling song structure analyses and comparison of H. maculaticollis

The song pattern of the MX population (Meixian County, Shaanxi, China) is presented in Fig. 10 and Audio S1. The calling song is composed of three parts of approximately 97.05 ± 24.87 s (mean ± SD; range = 72.18–121.92 s) ($N = 11$) duration (Fig. 10A). The first part of approximately 24.46 ± 1.29 s (mean ± SD; range = 23.17–25.75 s) duration is a relatively long series of sustained short echemes (Fig. 10B). In the frequency domain of Part 1, the power spectrum shows three main parts (F1, F2, F3) (Fig. 10C, D, E): F1 is between 3.45 and 5.43 kHz with a peak around 4.64 kHz; F2 is between 8.00 and 10.60 kHz with a peak around 9.04 kHz; and F3 is between 11.97 and 15.59 kHz with a peak around 15.00 kHz. Peaks F1 and F3 are the dominant frequencies with maximum amplitude. The second part of approximately 67.53 ± 22.64 s (mean ± SD; range = 44.89–90.17 s) duration generally comprises a series of ~10–16 phrases (Fig. 10A, F), and each phrase is typically

Table 4. AMOVA for testing the population structure of mainland China populations with mtDNA genes and that of East Asia populations with *COI* gene.

Gene(s)	Source of variation	d.f.	Sum of squares	Variance components	Percentage of variation	Fixation indices
COI + *COII* + *Cytb*	Among groups	5	1077.723	11.88673Va	81.83	Φ_{CT}:0.81829
	Among populations within groups	8	92.019	1.86135Vb	12.81	Φ_{SC}:0.94643
	Within populations	88	68.483	0.77822Vc	5.36	Φ_{ST}:0.70517
	Total	101	1238.225	14.52629		
COI	Among groups	5	647.731	6.62271Va	85.03	Φ_{CT}:0.85032
	Among populations within groups	9	39.452	0.56734Vb	7.28	Φ_{SC}:0.48666
	Within populations	103	61.639	0.59844Vc	7.68	Φ_{ST}:0.92316
	Total	117	748.882	7.78849		

Significance test: 1000 permutations; d.f.: degrees of freedom; all values were significant at $P < 0.01$.

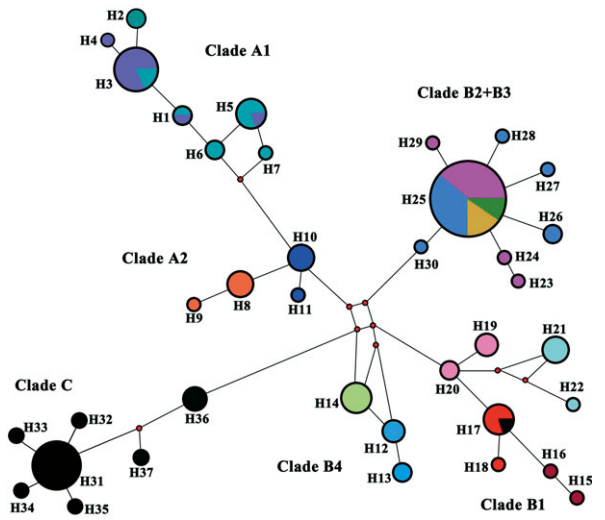

Fig. 7. Network profile based on the *COI* gene of China, Japan and South Korea populations. Each haplotype is represented by a circle. The size of the circle is proportional to that haplotype's frequency. Colours denote lineage membership and are the same as in Fig. 1. [Colour figure can be viewed at wileyonlinelibrary.com].

composed of ~6–7 echemes (Fig. 10F). In the frequency domain of Part 2, the power spectrum also shows three main parts (F1, F2, F3) (Fig. 10G, H, I): F1 is between 3.20 and 5.60 KHz with a peak around 4.74 KHz; F2 is between 6.00 and 6.90 kHz with a peak around 6.63 kHz; and F3 is between 13.00 and 16.00 kHz with a peak around 14.56 kHz. Peaks F1 and F3 are the dominant frequencies with maximum amplitude. The third part of approximately 5.06 ± 0.94 s (mean ± SD; range = 4.12–6.00 s) duration is the final phrase of the calling song, comprising ~6 echemes which are different with those in the phrases of the second part (Fig. 10J). In the frequency domain of Part 3, the power spectrum also shows three main parts (F1, F2, F3) (Fig. 10K, L, M): F1 is between 3.96 and 4.82 kHz with a peak around 4.64 kHz; F2 is between 6.10 and 7.00 kHz with a peak around 6.89 kHz; and F3 is between 12.58 and 15.59 kHz with a peak around 14.90 kHz. Peaks F1 and F3 are the dominant frequencies with maximum amplitude. Each phrase of Parts 1 and 2 is characterized by an increasing amplitude oscillation echeme at the beginning and a decreasing amplitude oscillation echeme at the end.

The domain frequency and duration of calling songs of the TM population (Tianmu Mountain, Zhejiang, China) showed no difference with that of the MX population (Figure S3). Nevertheless, significant variance of calling song structure was found in the QD population (Qingdao, Shandong, China) when compared with other populations of *H. maculaticollis* (Fig. 11). Specifically, the calling song is composed of four parts. The first part of approximately 4 ± 1.29 s (mean ± SD; range = 2.71–5.29 s) duration is a very short series of short echemes (Fig. 11A). The second part of about 61 ± 13.80 s (mean ± SD; range = 47.20–74.80 s) duration is a series of about ~7–10 phrases, and each phrase is typically composed of ~6–8 echemes (Fig. 11A). The third part of approximately 11.06 ± 1.94 s (mean ± SD; range = 11.12–13.00 s) duration is composed of only one phrase, comprising ~9–11 echemes which are different to those in the phrases of the second

Table 5. Genetic diversity and neutrality tests calculated for mainland China haplogroups based on mtDNA genes.

	NS	Nh	$H \pm$ SD	$\pi \pm$ SD	Tajima' D	Fu's F_s
Clade A1	58	8	0.772 ± 0.037	0.00248 ± 0.00157	1.66370	2.813
Clade A2	20	6	0.800 ± 0.067	0.00107 ± 0.00103	0.14548	−0.612
Clade B1	35	10	0.894 ± 0.026	0.00465 ± 0.00354	1.08491	2.844
Clade B2	36	6	0.308 ± 0.099	0.00027 ± 0.00088	−1.90505[a]	−4.158
Clade B3	41	9	0.356 ± 0.097	0.00027 ± 0.00114	−2.17514[a]	−9.408[a]
Clade B4	20	4	0.695 ± 0.079	0.00299 ± 0.00188	1.5105	3.114

[a]Significant value.
NS, number of samples; Nh, number of haplotypes; H, haplotype diversity; π, nucleotide diversity; SD, standard deviation.

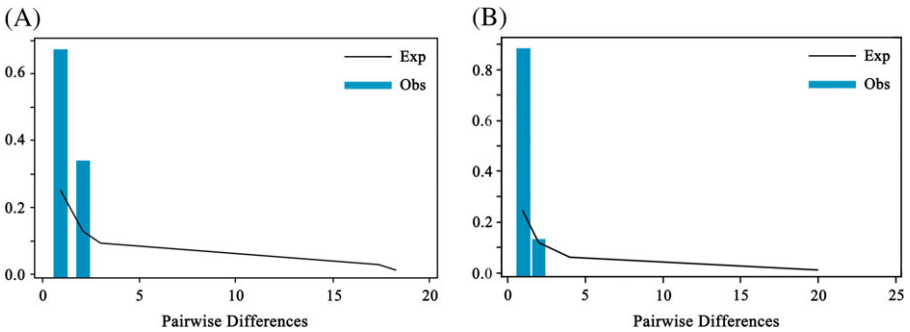

Fig. 8. Pairwise mismatch distribution for *Hyalessa maculaticollis*. (A) Clade B2; (B) Clade B3. X-axis, pairwise differences; Y-axis: frequency; Obs, observed distribution of pairwise difference; Exp, expected equilibrium distributions. [Colour figure can be viewed at wileyonlinelibrary.com].

Table 6. Intraspecific genetic distance of *Hyalessa maculaticollis* clades and interspecific genetic distance of *Hyalessa* based on the *COI* gene.

	Clade A1	Clade A2	Clade B1	Clade B2 + B3	Clade B4	Clade C	*H. ronshana*	*H. stratoria*	*H. wangi*
Clade A1	0.000–0.013								
CladeA2	0.008–0.018	0.000–0.005							
Clade B1	0.029–0.041	0.022–0.034	0.000–0.013						
Clade B2 + B3	0.025–0.037	0.020–0.029	0.007–0.017	0.000–0.005					
Clade B4	0.025–0.036	0.020–0.027	0.005–0.015	0.007–0.013	0.000–0.005				
Clade C	0.034–0.044	0.029–0.037	0.030–0.041	0.027–0.037	0.027–0.037	0.000–0.012			
H. ronshana	0.075–0.087	0.073–0.077	0.075–0.083	0.068–0.073	0.073–0.081	0.077–0.087	0.000–0.002		
H. stratoria	0.114–0120	0.108–0.110	0.110–0.116	0.106–0.112	0.108–0.110	0.108–0.114	0.120–0.122	0.000–0.000	
H. wangi	0.120–0.130	0.118–0.120	0.116–0.128	0.112–0.116	0.116–0.116	0.108–0.114	0.130–0.132	0.106–0.106	0.000–0.000

part (Fig. 11B). The fourth part of approximately 5 ± 0.50 s (mean ± SD; range = 4.50–5.50 s) duration is the final phrase of the calling song (Fig. 11B). This last phrase is composed of an isolated echeme followed by a sustained train of echemes (Fig. 11B). In the frequency domain, the power spectrum also shows four main parts (F1, F2, F3 and F4) (Fig. 11C, D): F1 and F2 are almost the same as that of the MX population; F3 is between 12.30 and 14.00 kHz with a peak around 13.15 kHz; and F4 is between 14.50 and 16.80 kHz with a peak around 15.65 kHz. Peaks F1, F3 and F4 are the dominant frequencies with maximum amplitude.

Comparison of calling song structure of populations of H. maculaticollis *and* 'H. fuscata'

The calling song structure of the so-called *H. fuscata* from South Korea (KOR) was compared with that of the MX, TM, QD and JAP populations of *H. maculaticollis* (Fig. 12A). Results show that there is no obvious difference in F1, F2 and F3 among the five populations ($P > 0.05$), except for the considerably lower values of F3 ($P < 0.05$) shown by the QD population of *H. maculaticollis* and the KOR population of '*H. fuscata*'. The time domain of Parts 1 and 3 both show remarkable differences ($P < 0.05$), but no distinct difference was found in Part 2 among the five populations (Fig. 12B). Besides, F4 is exclusively found in the calling songs of the QD and KOR populations. The results indicate that the QD population of *H. maculaticollis* and the KOR population of '*H. fuscata*' show no difference in calling song structure, with respect to the time duration and the domain frequency of the four parts ($P > 0.05$).

Acoustic playback experiments

The playback experiments showed that the calling songs of both the MX population and the QD population could elicit acoustic responses from males of the MX population (eight of 13 and six of 13 responded, respectively) (Fisher's exact test, $P = 0.6951$; Fig. 12C). Similarly, the calling songs of both the MX population and the QD population could elicit acoustic responses from males of the QD population (six of 13 and seven of 13 responded, respectively) (Fisher's exact test, $P = 1$; Fig. 12C; Figure S4). This confirms that the MX and QD populations belong to a single species, and also indicates that the KOR population, having the same calling song structure as the QD population but treated as *H. fuscata* by Lee (1999) and Puissant & Lee (2016), also belongs to same species – *H. maculaticollis*.

Discussion

Morphological variation and genetic divergence

Combining the results of morphological variation and genetic divergence analysis has allowed a more comprehensive

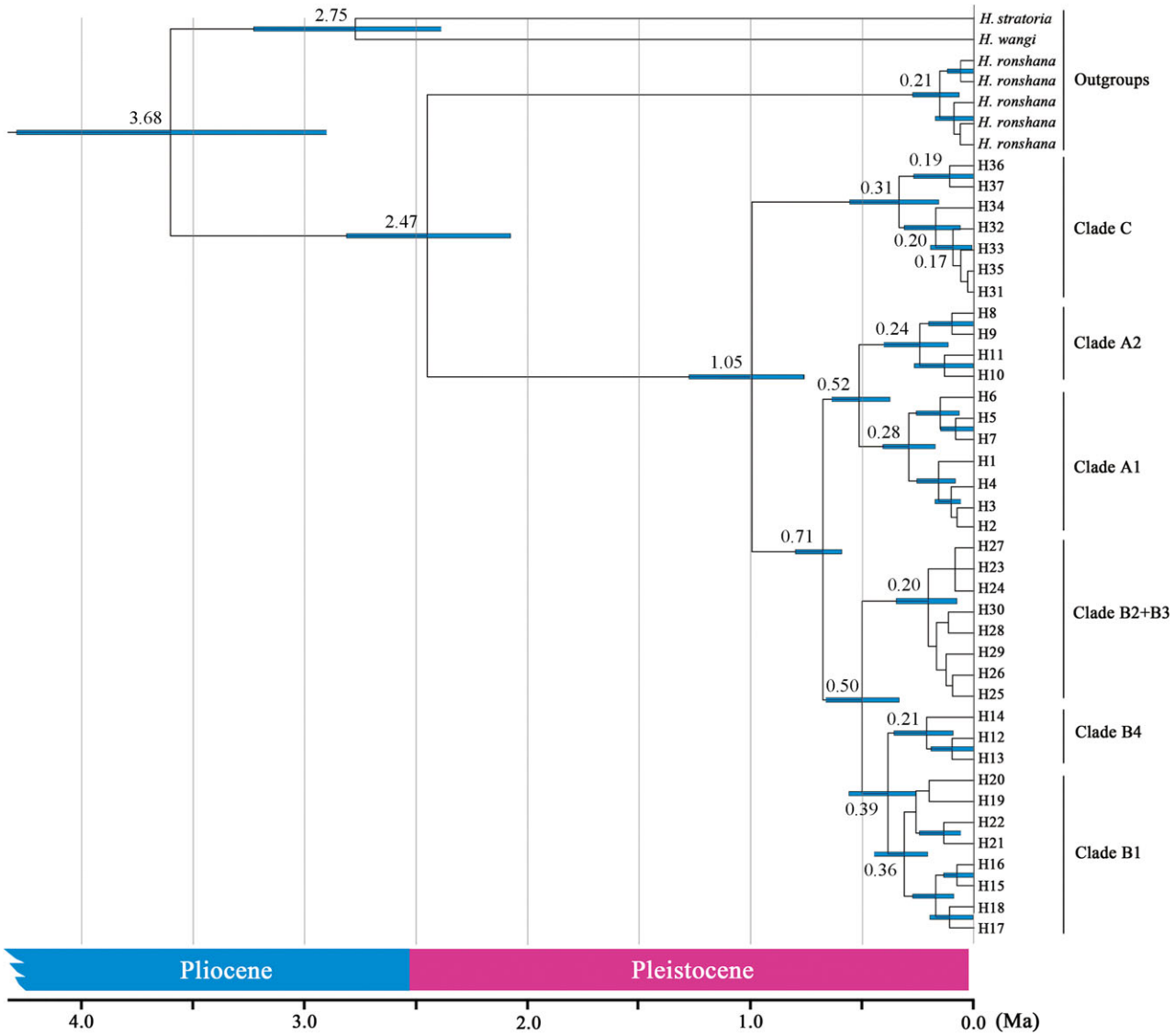

Fig. 9. The divergence time of *Hyalessa maculaticollis* and outgroup taxa based on *COI* gene. Estimates of divergence time are showed at nodes near branches. [Colour figure can be viewed at wileyonlinelibrary.com].

understanding of the genetic diversity of *H. maculaticollis*. Abundant intraspecific morphological variations in the mesonotum, male opercula and aedeagus of *H. maculaticollis* are consistent with high levels of genetic divergence. The populations on the mainland China are divided into two clades (A and B), and six haplogroups (clades A1–A2 and B1–B4). The variations of the markings on the mesonotum happened mainly in populations of clades B1–B3, which occurred mainly in northern and eastern China; the mesonotum of the remaining mainland China populations (clades B4 and A1–A2) all have five pairs of greenish spots. Regarding the male opercula, clades B2–B3 and populations DL and QD of Clade B1 have brown male opercula; populations TM and LS of Clade B1 have variegated male opercula, but populations with other haplogroups (clades B4 and A1–A2) have black male opercula. The S-shaped aedeagus is most common in *H. maculaticollis*, and the C-shaped variation occurs just in populations of clades B2–B3. The variation in the shape of aedeagus confirms that specimens with a C-shaped aedeagus, including the one formerly collected from Mt. Nanwutai of Xi'an, Shaanxi Province, are variants of *H. maculaticollis*. Surprisingly, the morphological characteristics of Clade B4 are more similar to those in Clade A, but the phylogenetic analyses strongly support that Clade B4 is more allied to other lineages of Clade B than to Clade A. This indicates that incongruence between the morphological variations and genetic divergence exists. Hayashi (2011) described abundant morphological variations in the populations occurring in Japan, which is also consistent with the result of high morphological/genetic divergence that we obtained herein.

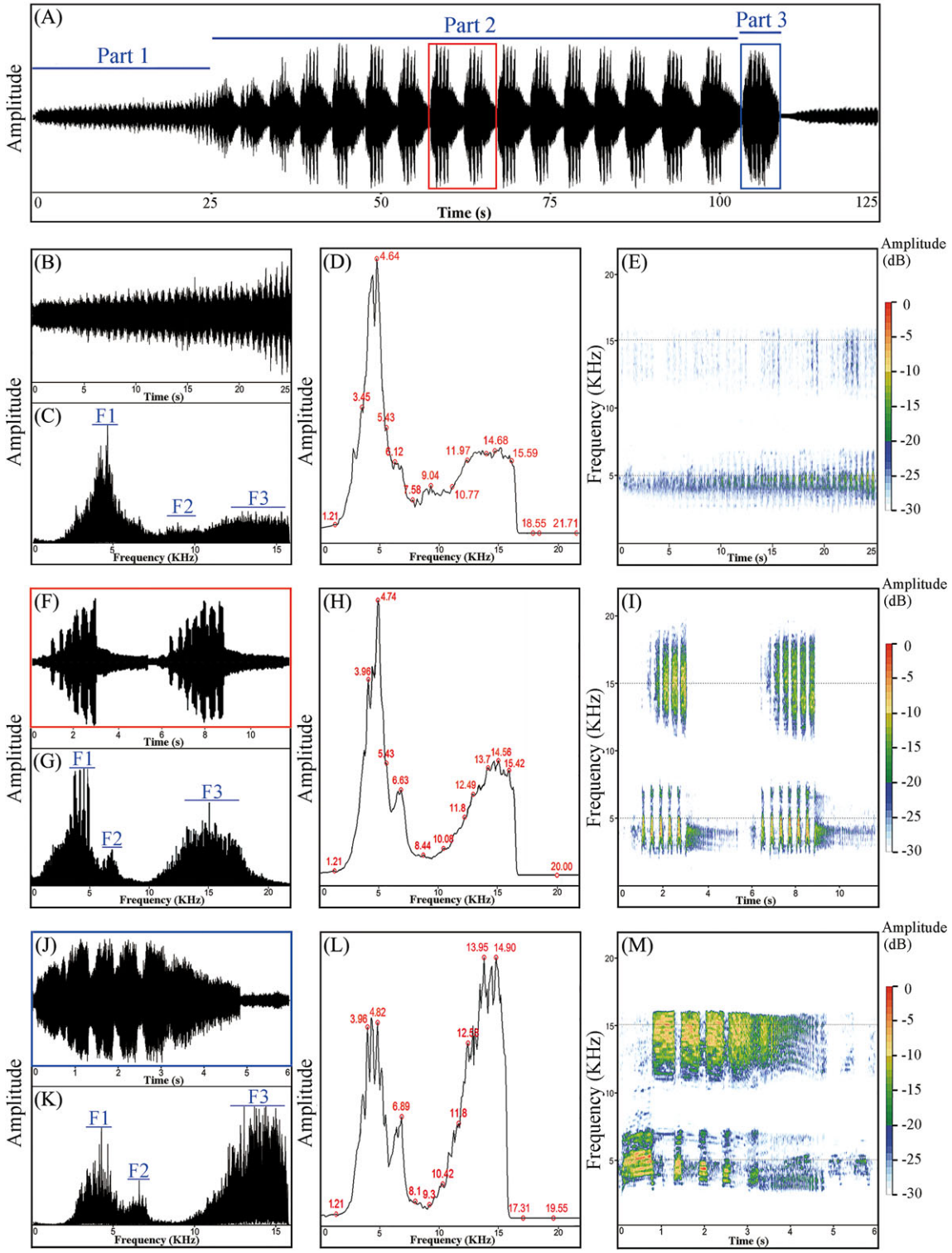

Fig. 10. Acoustic analyses of the calling song structure of *Hyalessa maculaticollis* from Meixian County (MX). (A) Oscillogram of a sequence of the calling song; (B) detailed oscillogram of Part 1; (C, D, E) power frequency spectrum of Part 1; (F) detailed oscillogram of partial phrases in Part 2 (marked by the red box in A); (G, H, I) power frequency spectrum of Part 2; (J) detailed oscillogram of Part 3 (marked by the blue box in A); (K, L, M) power frequency spectrum of Part 3. [Colour figure can be viewed at wileyonlinelibrary.com].

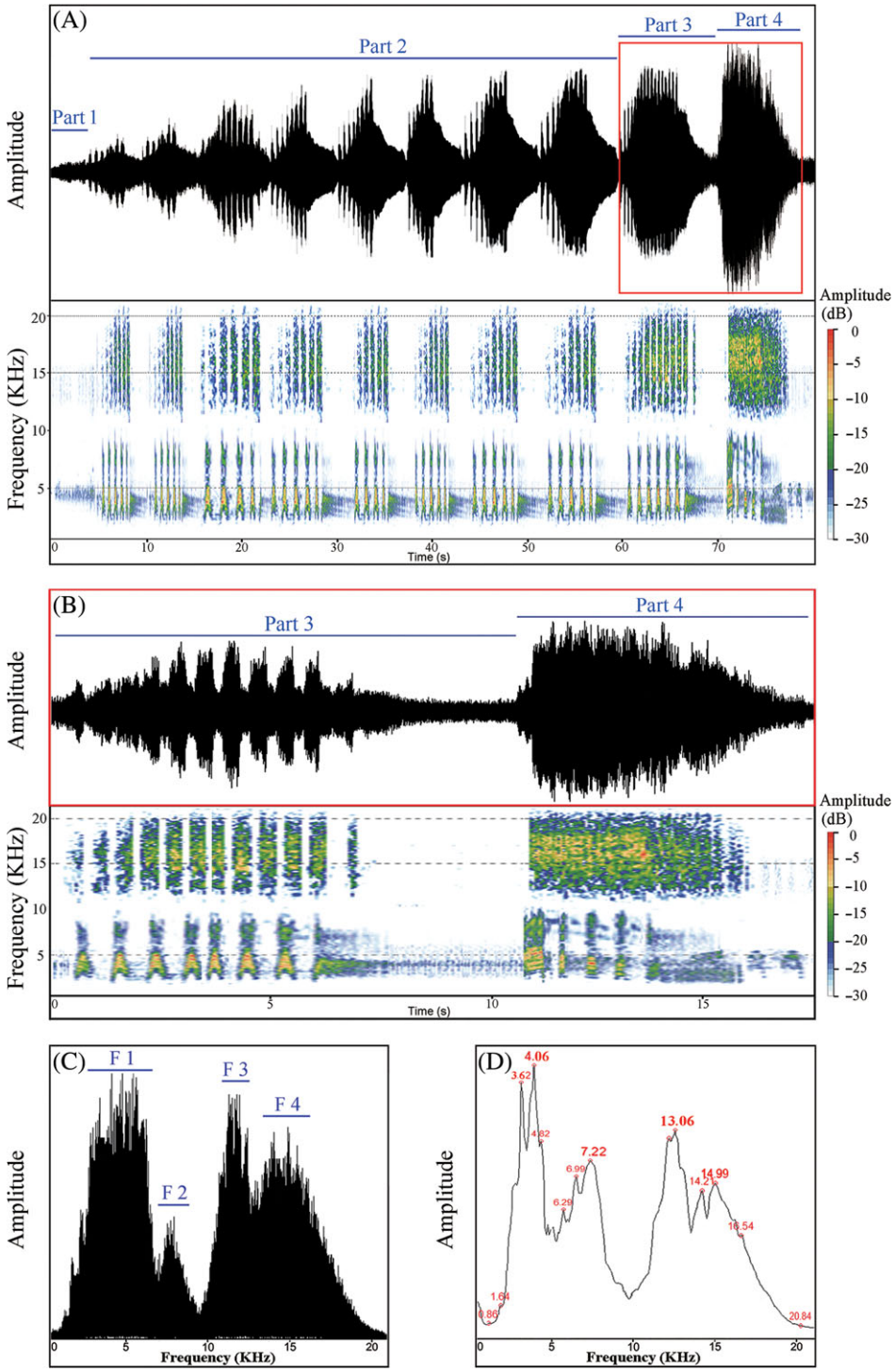

Fig. 11. Acoustic analyses of the calling song structure of *Hyalessa maculaticollis* from Qingdao (QD). (A) Oscillogram and spectrogram of a sequence of the calling song; (B) detailed oscillogram and spectrogram of Part 3 and Part 4 (marked by the red box in A); (C, D) power frequency spectrum with overlay of 174 spectra computed in the middle of the signal showing dominant frequencies marked by F1, F2, F3 and F4. [Colour figure can be viewed at wileyonlinelibrary.com].

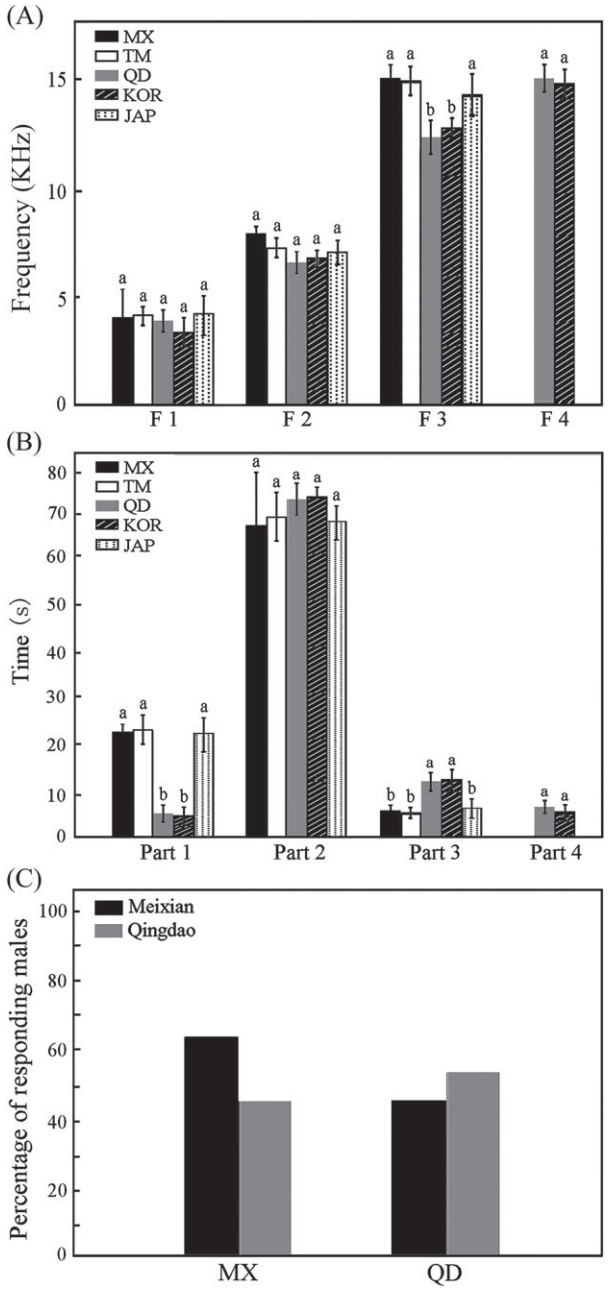

Fig. 12. Comparison of calling song structure of populations of *Hyalessa maculaticollis* and the so-called *H. fuscata* and related acoustic playback experiments. (A) Comparison of power frequency spectrum of F1, F2, F3 and F4 for five populations (data show mean ± SD). (B) Comparison of the duration of parts for five populations (data show mean ± SD). (C) Acoustic playback experiments: the efficiency of the two types of acoustic stimuli in eliciting acoustic responses from males. MX, natural male sounds of the MX population; QD, natural male sounds of the QD population.

Population differentiation and phylogeographical structure

The populations of *H. maculaticollis* are genetically highly structured across its range. Based on the *COI* locus, the populations of Japan (Clade C) diverged from the those of the mainland China (Fig. 7, Table 4). The phylogenetic trees show that Clade C is an independent lineage (Fig. 9, Figure S2). However, the genetic distance between the populations of Japan (Clade C) and northern China (Clade B2 + B3) is lower than Japan with almost all of the other mainland China populations (Table 6), and the genetic relationship of haplotype H36 of population HF (located in southwestern Japan) is close to the mainland China populations (Fig. 7). Therefore, we presume that the ancestor of *H. maculaticollis* may have invaded southwestern Japan from northern China. According to the result of the haplotype network (Fig. 7), all other haplotypes (H31–H37) are evolved from H36, indicating that the ancestral form spread (from southwest) northeastward. The populations of mainland China are more highly structured for concatenated datasets of mitochondrial genes; for example, populations XY, MX, NWT, HS, YC, YIC, XX, BBG and FUX occurring in northern China were further differentiated into two haplogroups (clades B2 and B3). Populations within each haplogroup are genetically similar, suggesting that sufficient gene flow has occurred within the same haplogroup and that restricted gene flow occurred between geographically separated haplogroups.

Historically, the glacial cycles of the Quaternary led to climatic oscillation and sea-level fluctuation, and had a significant effect on the evolutionary history and contemporary distribution patterns of current species in northern China, even though this area was not completely covered by ice sheets (Williams *et al.*, 1998; Zhang *et al.*, 2016). Results of our study indicate that the differentiation of populations of *H. maculaticollis* between mainland China and Japan took place ∼1.05 (95% CI = 00.89–1.30) Ma. The ECS land bridge formation and connection occurred between the Eurasian continent and the Japanese Islands ∼1.3–2.0 Ma (Kimura, 2003). Our estimated divergence time of populations between the mainland China and Japan is generally after this period. With the sea level increasing rapidly during the 'Ryukyu Coral Sea Stage' (0.2–1.3 Ma) (Kimura, 1996, 2003), the land bridge area became entirely submerged, and this vicariance event led to a long period of isolation. The gene flow of *H. maculaticollis* populations between the mainland China and Japan therefore could be blocked due to the isolation. The initial phase of divergence of populations from mainland China occurred at ∼0.71 Ma, which was during the early–middle Pleistocene (2.19–0.61 Ma). The rapid climate change and long-term low temperature should have resulted in population differentiation during this period. Subsequently, the divergence between clades A1 and A2 occurred at ∼0.52 Ma, and that between clades B2 + B3 and B1 + B4 occurred ∼0.50 Ma, both time points falling in the MIS 12 glaciations period (Zhao *et al.*, 2011). Therefore, we propose that climatic fluctuations in the Pleistocene were the main factor affecting the population differentiation of *H. maculaticollis*.

Our field investigations revealed that *H. maculaticollis* mainly occurs in the forests of low mountainous areas and the adjacent regions with flat terrain. We infer that geographical barriers on the mainland China influenced the phylogeographical structure of this species. In the Pleistocene, periodic expansions and contractions of the ice sheet led to species surviving in refugia during the glacial periods and subsequently expanding after the glaciations (Li *et al.*, 2009; Dai *et al.*, 2011). The two lineages of *H. maculaticollis* distributed on mainland China – clades A1–A2 and B1–B4 – might have contracted into isolated glacial refugia, in a similar way to the geometrid moth *Apocheima cinerarius* during the glacial periods (Liu *et al.*, 2015). Previous studies of potential quaternary glacial refugia in China have been conducted with respect to palynology, palaeoclimatology, palaeobotany and palaeozoology, and many potential refugia have been proposed, including the Qinling Mountains, Daba Mountains and the surrounding areas of the Sichuan Basin (Li *et al.*, 2009; Gao *et al.*, 2007; Chen *et al.*, 2011). According to the coalescent theory, the most frequent and widespread haplotype which occupies a central position in the network is expected to be the ancestral haplotype (Templeton *et al.*, 1995). In our study, the populations of Clade B2 which are distributed in the Qinling Mountains have the most widespread haplotype. We hypothesize that the Qinling Mountains were the refugium for *H. maculaticollis*, where this species survived periods of glaciation, and from which it subsequently expanded into the surrounding landscape. The Qinling Mountains might also have provided sufficient geographical isolation to hinder gene flow between populations of clades B2 and A1 located on different sides of the mountain range. There could also have been several ice-age refugia further north of the Qinling Mountains and some populations of *H. maculaticollis* survived there, as some areas (e.g. Beijing) in northern China belonged to the subtropical zone in the past (Zhu, 1973; Zhang, 2002). Given that populations YA, DJY and WC (located in the west of the Sichuan Basin) are closely related to populations FX, FP and NS (located on the south slopes of Qinling Mountains) (Fig. 1), mountainous regions around the Sichuan Basin might also have been ice-age refugia for *H. maculaticollis*. As one of the four great basins in China, the Sichuan Basin was likely to become a refugium for *H. maculaticollis* because of its surrounding mountain ranges, the Qinling–Daba Mountains and Loushan Mountains, which would have hindered glaciers and made the climate mild (Chen *et al.*, 2011). In addition, the surrounding mountain ranges might have effectively blocked the gene flow between those populations occurring within and without the Basin.

Given that many refugia in nonglaciated landscapes are associated with complex landscape topography, such as deep valleys besides mountain ranges (Médail & Diadema, 2009), the major valleys related to the Yangtze River and the Yellow River might also have been ice-age refugia for *H. maculaticollis*. According to the distribution pattern (Fig. 1) and haplotype network (Fig. 5A), the populations distributed in the area to the north of the Qinling Mountains might have expanded northward after the ice age, and then lineages of clades B2 and B3 might have become differentiated due to the lengthy separation caused by these valleys formed by the Yellow River. Similarly, the lineages of clades B4 (populations SNJ, BH) and A2 (populations HP, WF) might have been separated by the valleys caused by the Yangtze River. In contrast, populations of Clade B1 showed insignificant differentiation (i.e. higher values of haplotype and nucleotide diversity), indicating that sufficient gene flow occurred among those populations distributed in the flat terrains with low-altitude hills in eastern China.

The population of Tsushima Island (TI) is more closely related to the populations from East Asia mainland (Clade B1) than to those from Japan. A possible reason for this may be that sufficient gene flow occurred among populations distributed in mainland China and adjacent islands of the ECS. Wide extensions of continental shelf across the ECS were assumed to have been exposed, forming a large land bridge connecting the isolated continents of mainland China, Japan and probably the Korean Peninsula, during the LGM (~22 000 yr ago) of the last glacial period (Lambeck *et al.*, 2002), which might have resulted in the gene flow among *H. maculaticollis* populations on mainland China, Tsushima Island and other islands of the ECS.

The abovementioned results indicate that the climatic oscillation and terrain structure in East Asia influenced the population differentiation of *H. maculaticollis*, and the population structure has been shaped by the repeated exposure and submergence of the ECS land bridge (Zhang *et al.*, 2016).

Demographic history of the populations

The low haplotype diversity and low nucleotide diversity of *H. maculaticollis* indicate that a rapid demographic expansion has occurred in populations of clades B2–B3 (Table 5). The negative values resulting from Tajima's *D* test and Fu's F_s test indicate that the populations of these two haplogroups have experienced a recent population expansion. According to Rogers & Harpending (1992), an observed unimodal distribution of pairwise difference represents a population expansion, whereas an observed distribution of pairwise differences with many peaks curves indicates an equilibrium population. Accordingly, our results from analysis of the population size changes of *H. maculaticollis* suggest that the populations of clades B2–B3 experienced a population expansion (Fig. 8). The haplotype network shows that the haplogroup clades B2–B3 display a star-like pattern: H21 and H17 are located in the centre and derivatives are connected to them by short branches, respectively (Fig. 5). These star-like topologies also indicate the effect of a population expansion based on coalescence theory (Slatkin & Hudson, 1991). In contrast, the populations of Clade B1 have higher values for haplotype and nucleotide diversity. This character may be linked with the relatively smooth topography in eastern China, which is suitable for the survival of *H. maculaticollis* and allows more gene flow to occur.

Do populations distributed in China, Japan and Korea belong to one species?

Our morphological and molecular results reveal that populations of *H. maculaticollis* are genetically highly structured across its range, and that the Quaternary environmental fluctuations and geographical barriers had profound influences on the phylogeographical structure and demography of this species. We further discuss the long-standing controversy about whether the populations in China, Japan and the Korean Peninsula belong to one species, namely *H. maculaticollis*. Although effort has been made to amplify DNA of the KOR population, PCR amplification was not successful due to degradation of the DNA in very old specimens. Therefore, we only conducted molecular analyses on the populations from China and Japan. Based on the *COI* gene, intraspecific genetic distances (0.000–0.044) between all individuals of *H. maculaticollis* are lower than those between *Hyalessa* species (0.068–0.132). Previous studies found that the interspecific genetic distances of the cicada genera *Mogannia* and *Tettigettalna* were 0.066–0.233 and 0.027–0.116, respectively (Yang *et al.*, 2014; Nunes *et al.*, 2014). Marshall *et al.* (2009) suggested that the intraspecific genetic distance of the cicada *Kikihia subalpine* was 0.003–0.035. The genetic distance of individuals distributed on mainland China and Tsushima in Japan is 0.000–0.041, and that between individuals of Japan and mainland China is 0.027–0.044. This overlap demonstrates that the populations distributed in Japan are variants of *H. maculaticollis*. In particular, the Tsushima population is more closely related to the QD population occurring in the Shandong Peninsula of China, which indicates that this population is an intermediate form between populations of Japan and mainland China but not a hybrid, as described by Puissant & Lee (2016). Considering that Puissant & Lee (2016) conducted acoustic analyses of the calling song structure of '*H. fuscata*' occurring in South Korea and of *H. maculaticollis* distributed in Japan, we additionally analysed the calling song structure of *H. maculaticollis* populations occurring in central China from Meixian (MX) County, Tianmu (TM) Mountain and Qingdao (QD) City (abbreviated as '12 MX', '22 TM' and '21 QD' in Fig. 1). We discovered that the calling song structures of these populations showed acoustic differences with a few related populations distributed in Japan and the Korean Peninsula. However, our results indicated that there was no distinct difference in calling song structures between the QD population (*H. maculaticollis*) and the KOR population ('*H. fuscata*') in terms of duration and domain frequency of the four parts (Fig. 12A, B). Moreover, our acoustic playback experiments reveal that the KOR population has the same calling song structure as the QD population (Fig. 12C), further confirming that there should be no reproductive isolation between these two populations (Gerhardt & Huber, 2002; Drosopoulos & Claridge, 2006). Therefore, the proposal of synonymizing *H. fuscata* as *H. maculaticollis* by Hayashi & Saisho (2011) and Wang *et al.* (2014) is correct.

In addition, our results reveal that the ancestor of *H. maculaticollis* might have invaded into southwestern Japan and the Korean Peninsula from northern China, as the Korea Strait was substantially shallower during the late Pliocene (1.7–3.5 Ma) and the Japanese Island archipelago was an extension of the continent (Kitamura *et al.*, 2001; Kitamura & Kimoto, 2006). Although our effort to amplify DNA of the KOR population was not successful due to degradation of the DNA in very old specimens, we speculate that there is close affinity of populations occurring in the Korean Peninsula and the QD population in Shandong Province, China. This hypothesis needs to be confirmed based on further molecular phylogenetic analyses when materials from the Korean Peninsula become available. These results will be valuable for future studies of the phylogeographical relationships and evolution of other cicada species occurring in East Asia.

Supporting Information

Additional Supporting Information may be found in the online version of this article under the DOI reference: 10.1111/syen.12276

Figure S1. Phylogram reconstructed based on *COI* + *COII* + *Cytb* + *EF-1α* + *ITS* genes. Bayesian posterior probabilities and ML bootstrap values are indicated near tree branches.

Figure S2. Phylogram reconstructed based on the *COI* gene. Bayesian posterior probabilities and ML bootstrap values are indicated near tree branches.

Figure S3. Acoustic analyses of the calling song structure of *H. maculaticollis* from Tianmu (TM) Moutain. (A) Oscillogram of a sequence of the calling song. (B) Detailed spectrogram of the calling song. (C, D) Power frequency spectrum with overlay of the signal showing dominant frequencies marked by F1, F2 and F3.

Figure S4. Acoustic analyses of playback stimuli of the calling song structure of *H. maculaticollis* from Qingdao (QD) and the acoustic responses form males of the MX population. (A) Oscillogram of the acoustic stimuli and acoustic responses from males; the latter are marked by red boxes. (B) Oscillogram and spectrogram of the acoustic response (marked by the first red box in A). (C, D) Power frequency spectrum with overlay of the acoustic responses marked by F1, F2, F3 and F4, which correspond to a, b, c and d in B.

Audio S1. Male calling song of *H. maculaticollis* recorded in Meixian (MX) County, Shaanxi Province (WAV).

Acknowledgements

This research was supported by the National Natural Science Foundation of China (Grant No. 31572302) and Chinese Universities' Scientific Fund (Grant No. 2452017057). The authors would like to thank Professor John Richard Schrock (Emporia

State University, USA) for revising this manuscript and providing valuable comments. The authors declare no competing financial interests.

References

Arensburger, P., Buckley, T.R., Simon, C., Moulds, M. & Holsinger, K.E. (2004) Biogeography and phylogeny of the New Zealand cicada genera (Hemiptera: Cicadidae) based on nuclear and mitochondrial DNA data. *Journal of Biogeography*, **31**, 557–569.

Avise, J.C. (2000) *Phylogeography: The History and Formation of Species*. Harvard University Press, Cambridge, Massachusetts.

Bandel, H.J., Forster, P. & Röhl, A. (1999) Median-joining networks for inferring intraspecific phylogenies. *Molecular Biology and Evolution*, **16**, 37–48.

Brower, A.V.Z. (1994) Rapid morphological radiation and convergence among races of the butterfly *Heliconius erato* inferred from patterns of mitochondrial DNA evolution. *Proceedings of the National Academy of Sciences of the United States of America*, **91**, 6491–6495.

Brooks, S.P. & Gelman, A. (1998) General methods for monitoring convergence of iterative simulations. *Journal of Computational and Graphical Statistics*, **7**, 434–455.

Buckley, T.R., Simon, C. & Chambers, G.K. (2001) Phylogeography of the New Zealand cicada *Maoricicada campbelli* based on mitochondrial DNA sequences: ancient clades associated with Cenozoic environmental change. *Evolution*, **55**, 1395–1407.

Castresana, J. (2000) Selection of conserved blocks from multiple alignments for their use in phylogenetic analyses. *Molecular Biology and Evolution*, **17**, 540–552.

Chen, D.M., Kang, H.Z. & Liu, C.J. (2011) An overview on the potential quaternary glacial refugia of plants in China mainland. *Bulletin of Botanical Research*, **31**, 623–632.

Chou, I., Lei, Z., Li, L., Lu, X. & Yao, W. (1997) *The Cicadidae of China (Homoptera: Cicadoidea)*. Tianze Eldoneio, Hong Kong (in Chinese with English summary).

Cristiano, M.P., Cardoso, D.C., Fernandes-Salomão, T.M. & Heinze, J. (2016) Integrating paleodistribution models and phylogeography in the grass-cutting ant *Acromyrmex striatus* (Hymenoptera: Formicidae) in southern lowlands of South America. *PLoS ONE*, **11**, e0146734.

Dai, C.Y., Zhao, N., Wang, W.J. *et al.* (2011) Profound climatic effects on two east Asian black-throated tits (Ave: Aegithalidae), revealed by ecological niche models and phylogeographic analysis. *PLoS One*, **6**, e29329.

De Jong, M.A., Wahlberg, N., Van Eijk, M., Brakefield, P.M. & Zwaan, B.J. (2011) Mitochondrial DNA signature for range-wide populations of *Bicyclus anynana* suggests a rapid expansion from recent refugia. *PLoS One*, **6**, e21385.

Distant, W.L. (1905) Rhynchotal notes – XXVIX. *Annals and Magazine of Natural History*, **16**, 553–557.

Drosopoulos, S. & Claridge, M.F. (2006) *Insect Sounds and Communication: Physiology, Behaviour, Ecology and Evolution*. CRC Press Taylor & Francis Group, Boca Raton, Florida.

Drummond, A.J. & Rambaut, A. (2007) BEAST: Bayesian evolutionary analysis by sampling trees. *BMC Evolutionary Biology*, **7**, 214.

Excoffier, L. & Lischer, H.E. (2010) Arlequin suite ver 3.5: a new series of programs to perform population genetics analyses under Linux and Windows. *Molecular Ecology Resources*, **10**, 564–567.

Gao, L.M., Möller, M., Zhang, X.M. *et al.* (2007) High variation and strong phylogeographic pattern among cpDNA haplotypes in *Taxus wallichiana* (Taxaceae) in China and North Vietnam. *Molecular Ecology*, **16**, 4684–4698.

Gerhardt, H.C. & Huber, F. (2002) *Acoustic Communication in Insects and Anurans: Common Problems and Diverse Solutions*. University of Chicago Press, Chicago, Illinois.

Guindon, S. & Gascuel, O. (2003) A simple, fast, and accurate algorithm to estimate large phylogenies by maximum likelihood. *Systematic Biology*, **52**, 696–704.

Hall, T.A. (1999) BioEdit: a user-friendly biological sequence alignment editor and analysis program for windows 95/98/NT. *Nucleic Acids Symposium Series*, **41**, 95–98.

Hayashi, M. (2011) Preliminary notes on some taxonomic changes in Japanese Cicadidae. *Cicada*, **20**, 2–5 (in Japanese with English summary).

Hayashi, M. & Saisho, Y. (2011) *The Cicadidae of Japan*. Seibundo-Shinkosha, Tokyo (in Japanese).

Hewitt, G.M. (1996) Some genetic consequences of ice ages, and their role in divergence and speciation. *Biological Journal of the Linnean Society*, **58**, 247–276.

Hewitt, G.M. (2000) The genetic legacy of the quaternary ice ages. *Nature*, **405**, 907–913.

Hewitt, G.M. (2004) Genetic consequences of climatic oscillations in the quaternary. *Philosophical Transactions of the Royal Society of London B*, **359**, 183–195.

Hill, K.B.R., Simon, C., Marshall, D.C. & Chambers, G.K. (2009) Surviving glacial ages within the biotic gap: phylogeography of the New Zealand cicada Maoricicada campbelli. *Journal of Biogeography*, **36**, 675–692.

Holt, B.G., Lessard, J.P., Borregaard, M.K. *et al.* (2013) An update of Wallace's zoogeographic regions of the World. *Science*, **339**, 74–77.

Jeanmougin, F., Thompson, J.D., Gouy, M., Higgins, D.G. & Gibson, T.J. (1998) Multiple sequence alignment with Clustal X. *Trends in Biochemical Sciences*, **23**, 403–405.

Ji, Y.J., Zhang, D.X. & He, L.J. (2003) Evolutionary conservation and versatility of a new set of primers for amplifying the ribosomal internal transcribed spacer regions in insects and other invertebrates. *Molecular Ecology Notes*, **3**, 581–585.

Jiang, Y., Kang, M., Zhu, Y. & Xu, G. (2007) Plant biodiversity patterns on Helan ountain, China. *Acta Oecologica-inter National Journal of Ecology*, **32**, 125–133.

Kimura, M. (1996) [Quaternary paleogeography of the Ryukyu Arc.] *Journal of Geography*, **105**, 259–185 (in Japanese with English summary).

Kimura, M. (2003) Land connections between Eurasian continent and Japanese Islands-related to human migration. *Migration and Diffusion*, **4**, 14–33.

Kitamura, A. & Kimoto, K. (2006) History of the inflow of the warm Tsushima current into the sea of Japan between 35 and 08 Ma. *Palaeogeography, Palaeoclimatology, Palaeoecology*, **236**, 355–366.

Kitamura, A., Takano, O., Takada, H. & Omote, H. (2001) Late Pliocene-early Pleistocene paleoceanographic evolution of the sea of Japan. *Palaeogeography, Palaeoclimatology, Palaeoecology*, **172**, 81–98.

Lalitha, S. (2000) Primer premier 5. *Biotech Software & Internet Report*, **1**, 270–272.

Lambeck, K., Esat, T.M. & Potter, E.K. (2002) Links between climate and sea levels for the past three million years. *Nature*, **419**, 199–206.

Lanfear, R., Calcott, B., Ho, S.Y.W. & Guindon, S. (2012) PartitionFinder: combined selection of partitioning schemes and substitution models for phylogenetic analyses. *Molecular Biology and Evolution.*, **29**, 1695–1701.

Lee, Y.J. (1999) A list of Cicadidae (Homoptera) in Korea. *Cicada*, **15**, 1–16.

Lee, Y.J. (2010) Cicadas (Insecta: Hemiptera: Cicadidae) of Mindanao, Philippines, with the description of a new genus and a new species. *Zootaxa*, **2351**, 14–28.

Li, S.H., Yeung, C.K.L., Feinstein, J., Han, L., Le, M.H., Wang, C.X. & Ding, P. (2009) Sailing through the Late Pleistocene: unusual historical demography of an East Asian endemic, the Chinese hwamei (*Leucodioptron canorum canorum*), during the last glacial period. *Molecular Ecology*, **18**, 622–633.

Librado, P. & Rozas, J. (2009) DnaSP v5: a software for comprehensive analysis of DNA polymorphism data. *Bioinformatics*, **25**, 1451–1452.

Liu, S.X., Jiang, N., Xue, D.Y. *et al.* (2015) Evolutionary history of *Apocheima cinerarius* (Lepidoptera: Geometridae), a female flightless moth in northern China. *Zoologica Scripta*, **45**, 160–174.

Maekawa, K., Kon, M., Araya, K. & Matsumoto, T. (2001) Phylogeny and biogeography of wood-feeding cockroaches, genus *Salganea* Stål (Blaberidae: Panesthiinae), in southeast Asia based on mitochondrial DNA sequences. *Journal of Molecular Evolution*, **53**, 651–659.

Marshall, D.C., Slon, K., Cooley, J.R., Hill, K.B. & Simon, C. (2008) Steady Plio-Pleistocene diversification and a 2-million-year sympatry threshold in a New Zealand cicada radiation. *Molecular Phylogenetics and Evolution*, **48**, 1054–1066.

Marshall, D.C., Hill, K.B., Fontaine, K.M., Buckley, T.R. & Simon, C. (2009) Glacial refugia in a maritime temperate climate: cicada (*Kikihia subalpina*) mtDNA phylogeography in New Zealand. *Molecular Ecology*, **18**, 1995–2009.

Marshall, D.C., Hill, K.B., Cooley, J.R. & Simon, C. (2011) Hybridization, mitochondrial DNA phylogeography, and prediction of the early stages of reproductive isolation: lessons from New Zealand cicadas (genus *Kikihia*). *Systematic Biology*, **60**, 482–502.

Marshall, D.C., Hill, K.B., Marske, K.A., Chambers, C., Buckley, T.R. & Simon, C. (2012) Limited, episodic diversification and contrasting phylogeography in a New Zealand cicada radiation. *BMC Evolutionary Biology*, **12**, 177.

Médail, F. & Diadema, K. (2009) Glacial refugia influence plant diversity patterns in the Mediterranean Basin. *Journal of Biogeography*, **36**, 1333–1345.

Moulds, M.S. (2005) An appraisal of the higher classification of cicadas (Hemiptera: Cicadoidea) with special reference to the Australian fauna. *Records of the Australian Museum*, **57**, 375–446.

Moulds, M.S. (2012) A review of the genera of Australian cicadas (Hemiptera: Cicadoidea). *Zootaxa*, **3287**, 1–262.

Nunes, V.L., Mendes, R., Marabuto, E. *et al.* (2014) Conflicting patterns of DNA barcoding and taxonomy in the cicada genus *Tettigettalna* from southern Europe (Hemiptera: Cicadidae). *Molecular Ecology Resources*, **14**, 27–38.

Owen, C.L., Marshall, D.C., Hill, K.B. & Simon, C. (2016) How the Aridification of Australia structured the biogeography and influenced the diversification of a large lineage of Australian cicadas. *Systematic Biology*, **66**, 1–21.

Pinto-Juma, G.A., Quartau, J.A. & Bruford, M.W. (2008) Population structure of *Cicada barbara* Stål (Hemiptera, Cicadoidea) from the Iberian Peninsula and Morocco based on mitochondrial DNA analysis. *Bulletin of Entomological Research*, **98**, 15–25.

Puissant, S. & Lee, Y.J. (2016) Description of a new species of the genus *Hyalessa* China (Hemiptera: Cicadidae: Sonatini) from Yunnan, China, with a key to the species of *Hyalessa* and a calling song analysis for two *Hyalessa* species. *Zootaxa*, **4114**, 434–446.

Puissant, S. & Sueur, J. (2010) A hotspot for Mediterranean cicadas (Insecta: Hemiptera: Cicadidae): new genera, new species and new songs from southern Spain. *Systematics and Biodiversity*, **8**, 555–574.

Rambaut, A. & Drummond, A.J. (2009) *Tracer Version1.5.0*. [WWW document]. URL http://beast.bio.ed.ac.uk/software/tracer/ [accessed on 10 March 2015]

R Development Core Team (2011) *R: A Language and Environment for Statistical Computing*. R Foundation for Statistical Computing, Vienna.

Rogers, A.R. & Harpending, H. (1992) Population growth makes waves in the distribution of pairwise genetic differences. *Molecular Biology and Evolution*, **9**, 552–569.

Ronquist, F. & Huelsenbeck, J.P. (2003) MrBayes3: Bayesian phylogenetic inference under mixed models. *Bioinformatics*, **19**, 1572–1574.

Scarpassa, V.M., Figueiredo, A.S. & Alencar, R.B. (2015) Genetic diversity and population structure in the Leishmania guyanensis vector *Lutzomyia anduzei* (Diptera, Psychodidae) from the Brazilian Amazon. *Infection, Genetics and Evolution*, **31**, 312–320.

Simon, C., Frati, F., Beckenbach, A., Crespi, B., Liu, H. & Flook, P. (1994) Evolution, weighting and phylogenetic utility of mitochondrial gene sequences and a compilation of conserved PCR primers. *Annals of the Entomological Society of America*, **87**, 651–701.

Slatkin, M. & Hudson, R.R. (1991) Pairwise comparisons of mitochondrial DNA sequences in stable and exponentially growing populations. *Genetics*, **129**, 555–562.

Stål, C. (1870) Hemiptera insularum Philippinarum. Bidrag till Philippinska öarnes Hemipter–fauna. *Öfversigt af Kongl. Vetenskaps-Akademiens Förhandlingar*, **27**, 607–776.

Sueur, J., Aubin, T. & Simonis, C. (2008) Seewave, a free modular tool for sound analysis and synthesis. *Bioacoustics*, **18**, 213–226.

Tamura, K., Stecher, G., Peterson, D., Filipski, A. & Kumar, S. (2013) MEGA6: molecular evolutionary genetics analysis version 6.0. *Molecular Biology and Evolution*, **30**, 2725–2729.

Templeton, A.R., Routman, E. & Phillips, C.A. (1995) Separating population structure from population history: a cladistic analysis of the geographical distribution of mitochondrial DNA haplotypes in the tiger salamander, *Ambystoma tigrinum*. *Genetics*, **140**, 767–782.

Thompson, J.D., Gibson, T.J., Plewniak, F., Jeanmougin, F. & Higgins, D.G. (1997) The Clustal X windows interface: flexible strategies for multiple sequence alignment aided by quality analysis tools. *Nucleic Acids Research*, **25**, 4876–4882.

Wang, X., Hayashi, M. & Wei, C. (2014) On cicadas of *Hyalessa maculaticollis* complex (Hemiptera, Cicadidae) of China. *ZooKeys*, **369**, 25–41.

Williams, M.A.J., Dunkerley, D.L., De Deckker, P., Kershaw, A.P. & Chappel, J. (1998) *Quaternary Environments*. Arnold, London.

Xia, X. (2013) DAMBE5: a comprehensive software package for data analysis in molecular biology and evolution. *Molecular Biology and Evolution.*, **30**, 1720–1728.

Yang, M.S., Chen, X., Huo, W.X. & Wei, C. (2014) Morphological variation versus genetic divergence: a taxonomic implication for *Mogannia* species (Cicadidae: Cicadinae). *Systematics and Biodiversity*, **12**, 1–17.

Ye, Z., Zhu, G.P., Damgaard, J., Chen, X., Chen, P.P. & Bu, W.J. (2016) Phylogeography of a semiaquatic bug, *Microvelia horvathi* (Hemiptera: Veliidae): an evaluation of historical, geographical and ecological factors. *Scientific Reports*, **6**, 21932.

Zahniser, J.N. & Dietrich, C.H. (2015) Phylogeny, evolution, and historical biogeography of the grassland leafhopper tribe Chiasmini (Hemiptera: Cicadellidae: Deltocephalinae). *Zoological Journal of the Linnean Society*, **175**, 473–495.

Zhang, D.L., Ye, Z., Yamada, K., Zhen, Y.H., Zheng, C.G. & Bu, W.J. (2016) Pleistocene sea level fluctuation and host plant habitat requirement influenced the historical phylogeography of the invasive species *Amphiareus obscuriceps* (Hemiptera: Anthocoridae) in its native range. *BMC Evolutionary Biology*, **16**, 174.

Zhang, R.Z. (2002) Geological events and mammalian distribution in China. *Acta Zoologica Sinica*, **2**, 141–153.

Zhao, J.D., Shi, Y.F. & Wang, J. (2011) Comparison between quaternary glaciations in China and the marine oxygen isotope stage (MIS): an improved schema. *Acta Geographica Sinica*, **7**, 867–884.

Zhu, G.P., Ye, Z., Du, J. *et al.* (2016) Range wide molecular data and niche modeling revealed the Pleistocene history of a global invader (*Halyomorpha halys*). *Scientific Reports*, **6**, 23 192.

Zhu, K.Z. (1973) [A preliminary study on the climatic fluctuations during the last 5000 years in China.] *Scientia Sinica*, **16**, 226 (in Chinese).

Accepted 1 October 2017